Chapter 7

NMES Cycling experiments

7.1 Effect of 5 minutes continuous cycling on the development of crank torque

7.1.1 Introduction

The first cycling session consisted of 5 minutes continuous cycling using stimulation of only the right quadriceps muscles. Stimulation commenced at a crank angle of 300 deg and ceased at 20 deg after TDC. Data from one subject was corrupted during the collection process leaving measures from six subjects available. Figure 7.1.1.1 illustrates how a typical nett crank torque - angle curve changed during the 5 minutes of this experiment. Nett torques are the result of subtracting torque measured during passive cycling from measurements taken while the muscles are being stimulated. The crank cycle can be broken down into an active phase (approximately 320 to 90 deg) where quadriceps contractions applied torque to the crank, and an inactive phase (approximately 90 to 320 deg) where the muscles were relaxed and not applying torque to the crank. The non-zero torque levels during the inactive phase are important for understanding the results of this section, however hypothesised mechanisms explaining these results will not be proposed until Section 7.2.

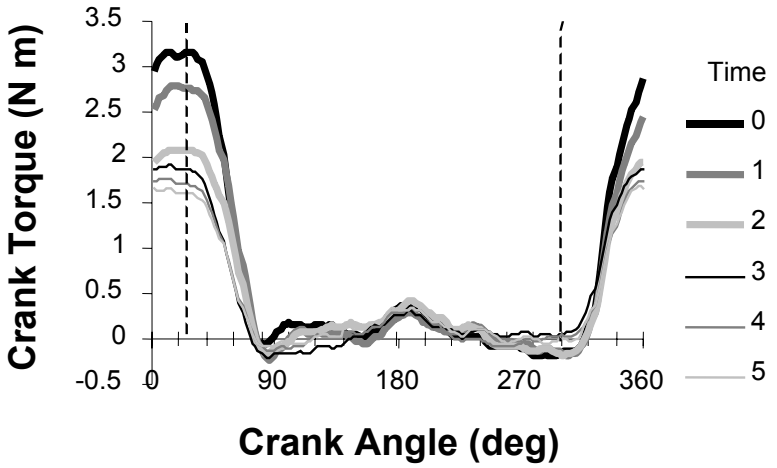

Figure 7.1.1.1 Typical crank torque – angle curve for a single subject with stimulation firing angles between 300 and 20 deg. Vertical dotted lines represent the timing of stimulation onset and cessation. Numbers for each curve represent the time of data collection (in minutes) within the 5 minutes continuous cycling.

7.1.2 Changes in crank torque with quadriceps fatigue

Over the course of 5 minutes, muscle fatigue caused average power output to drop nearly 50% from an average of 2.64 down to 1.33 W (Figure 7.1.2.1). The drop in power output was most evident during the first two minutes of cycling and tended to plateau thereafter. The cycling power outputs achieved in this study are very low compared to most previously reported studies on NMES cycling for SCI individuals (eg Faghri et al., 1992: 17 W). The present data, however, represent the stimulation of only one quadriceps muscle, rather than bilateral stimulation of the quadriceps, hamstrings and gluteal muscles.

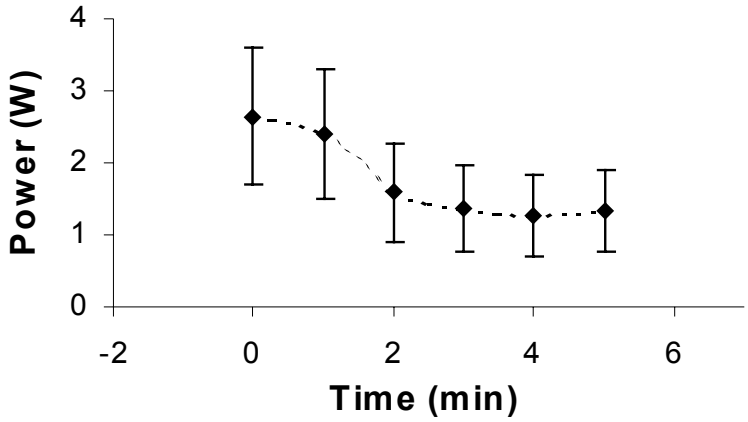

Figure 7.1.2.1 Change in power output during the course of five minutes continuous cycling using stimulation of just the right quadriceps muscles.

Although the torque and hence power output declined throughout the cycling period (Figure 7.1.1.1), there was little change in the overall shape of the torque-angle curves (Figure 7.1.2.2). Time 4 is the only curve that differs from the others and this was affected by a single subject that fatigued more than the rest. If this subject were removed from the calculation of the time 4 average, then this curve would be superimposed over the others.

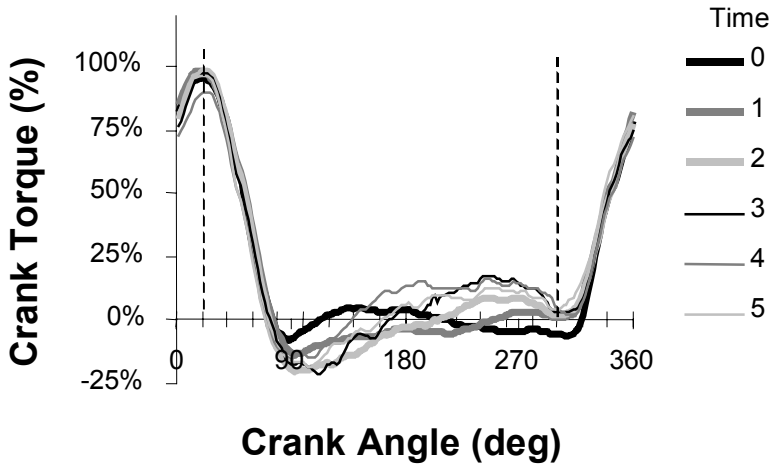

Figure 7.1.2.2 Torque patterns averaged for each subject and normalised against peak torque at time zero. Vertical dotted lines represent the timing of stimulation onset and cessation. Numbers for each curve represent the time of data collection (in minutes) within the 5 minutes continuous cycling.

To test the general shape of the torque curves in Figure 7.1.1.1, the average power output, crank angle where torque was maximum, and angles where 50% peak torque was reached in both the ascending and descending phases were analysed for each minute of the experiment. A multivariate, repeated measures ANOVA was performed with six levels used for time throughout the fatigue protocol (Table 7.1.2.1). Only the average power output, determined by the area under the torque - angle curve, generated a significant change. All other variables representing the timing of the curve showed no significant change. Although the number of subjects was small (n=6), the high p values (0.770, 0.686, 0.246) and consistency over time (Table 7.1.2.1, Figure 7.1.2.2) increase the confidence that there really was no demonstrable change in the timing of torque responses with fatigue.

Table 7.1.2.1 Changes in measured crank torque with fatigue.

	Time (minutes)						Significance
	0	1	2	3	4	5	
Power[1]	2.6 (1.0)	2.4 (0.9)	1.6 (0.7)	1.4 (0.6)	1.3 (0.6)	1.3 (0.6)	0.001
Up Angle[2]	345.3 (8.4)	345.7 (6.1)	347.0 (8.5)	348.3 (10.5)	346.8 (8.4)	345.3 (7.6)	0.770
Max Angle[3]	19.3 (8.8)	19.3 (6.2)	21.7 (5.3)	21.0 (5.9)	23.3 (7.3)	18.7 (13.2)	0.686
Down Angle[4]	50.7 (7.8)	53.0 (7.0)	54.0 (6.1)	53.3 (7.2)	52.2 (6.7)	51.0 (7.1)	0.246

Data represent the mean and one standard deviation from all subjects.

1 Power is the average power calculated from five revolutions in each trial

2 Up Angle is the crank angle where torque reached 50% of its peak value while rising in response to stimulation onset

3 Max Angle is the crank angle where torque reached its peak value

4 Down Angle is the crank angle where torque reached 50% of its peak value while declining in response to stimulation cessation

7.1.3 Comparison between measured and modelled crank torques

The NMES cycling model developed in Chapter 4 was customised to fit anthropometric data for each subject, and amplitude normalised to produce a maximum crank torque of 100%. It will be shown in Section 7.2.1 that there was little difference between subjects in the modelled crank torque curves. Consequently, only a mean modelled curve will be used for all figures within the present section.

The NMES cycling model generally provided very good matches to the experimental data with the mean correlation between measured and modelled torques averaging 0.85 (Figure 7.1.3.1). Only the torque applied to the crank will be examined in this section and no attempt made to discuss why the model differed from measured values. Section 7.2 will later examine vertical and horizontal components of pedal forces in order to better test the model's performance, and to suggest causes of poorer correlations.

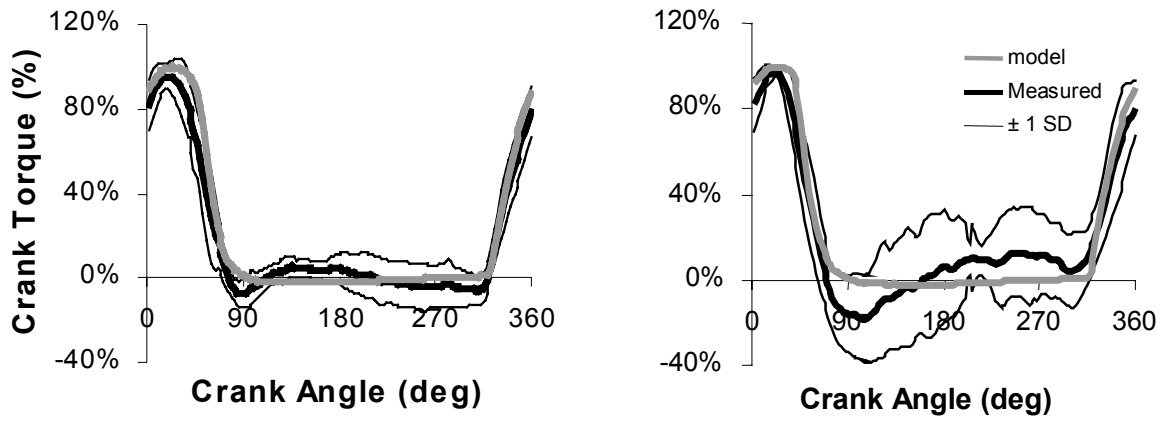

Time 0 Time 5

Figure 7.1.3.1 Measured and modelled crank torques at the beginning and end of five minutes cycling using NMES to the right quadriceps muscles.

Measured crank torques had the passive torque subtracted before comparison with the model, so that segment inertial values could be eliminated from the model. Small movements of subjects in their chair would have changed the passive torque-angle relationship and therefore affected measured nett torques. Since passive data were available only at the beginning and end of the 5 minute period, and these may not have been the same, it was decided to compare results calculated using both passive periods. A two-way analysis of variance with repeated measures was performed for correlation values using the six levels of time during the fatigue test and two different passive levels, collected before and after the active cycling period. The second passive cycling period was not available for one subject, leaving only five complete data sets for the ANOVA (Figure 7.1.3.2). This left insufficient subjects to perform multivariate tests within the ANOVA, hence only univariate results will be reported below.

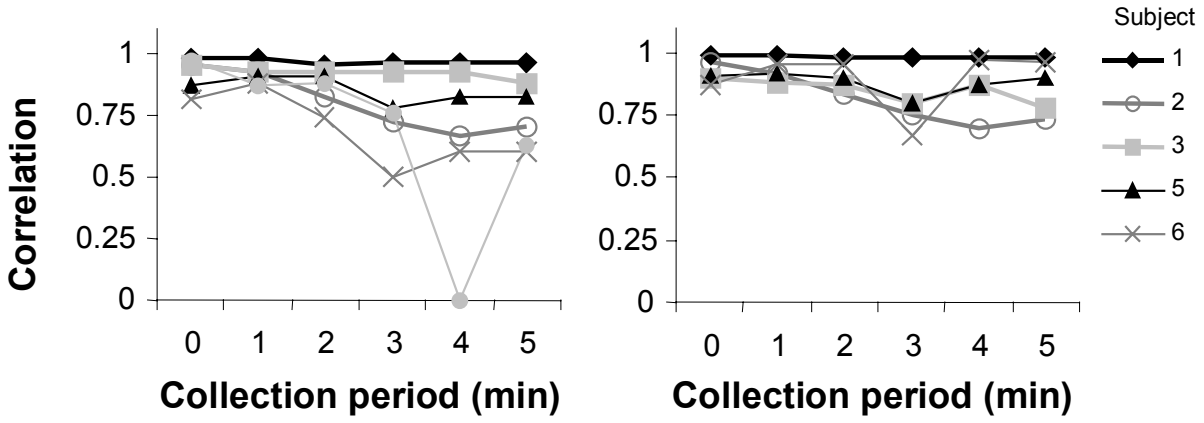

a) b)

Figure 7.1.3.2 Correlations between measured and modelled crank torques throughout the course of five minutes continuous cycling, calculated using passive levels taken before and after the active cycling period.

a) Nett torques calculated from passive data measured before the active cycling period.

b) Nett torques calculated from passive data measured after the active cycling period.

Some decline in correlation over time was to be expected from the decline in amplitude with fatigue because this increases the percentage error in the signal. Some reduction in correlation would also be expected because, as time increased, there was more likely to have been movement of the subject changing the passive torque levels. There was a significant trend for correlations to decline over the duration of the test (Figure 7.1.3.2, $p = 0.047$). One subject (6) demonstrated declining passive levels when the first passive level was used, however this trend was reversed when the second passive level was used (Figure 7.1.3.2). While this suggests that this subject was moving during the test so that the initial passive levels became more inappropriate, this trend was not evident for other subjects. It can be seen from Figure 7.1.3.2 that a number of subjects produced similar declines in correlation when calculated with both passive torque levels. Therefore, the ANOVA found no significant effect for the passive measurement used ($p = 0.41$) or interaction between passive level × time ($p = 0.31$). If changing passive levels had caused the declining correlations, then the ANOVA would have been expected to produce a significant interaction with correlations declining after the first passive measurement and improving towards the second passive trial.

Subject (7) produced relatively less torque than the other subjects and this, together with apparent muscle fatigue and moving of passive levels, resulted in a correlation of 0.0 for time 4. The results for Subject 7 were solely responsible for time 4 appearing different to the other times in Figure 7.1.2.2. It appeared that, for this trial the nett torque generated in response to stimulation was less than the change in passive levels during the inactive phase of each crank revolution. Unfortunately, there was no second passive trial available for this subject to test whether decline in correlation was the result of changing passive levels or increased noise to signal ratio.

Figures 7.1.1.1 and 7.1.3.1 show that, as fatigue progressed, a constant amount of error during the inactive phase (between 90 and 320 deg) would have become relatively larger in proportion to the active torque developed. This effect was particularly evident during the passive phase between 90 and 320 deg and must have contributed to the decline in correlations recorded as time progressed.

The change in correlations over time can therefore be attributed to either increasing error from changing passive torques, changes in the error to signal ratio, or in a change in the pattern of torque development. The first possibility is likely to have contributed, however the effect was variable between subjects. Analysis of the timing of torque events in Section 7.1.2 and visual inspection of Figure 7.1.2.2 suggest that the last option is unlikely to be significant. There is no evidence to suggest that the timing and relative shape of torque production changed over time. This conclusion is consistent with the findings from isometric contractions described in Section 5.1.2. Therefore, it seems likely that the largest contribution to decreasing correlations over time comes from the decrease in signal to error ratio over time. This decrease results from a reduction of peak torque in relation to the magnitude of differences between measured and modelled torque during the inactive phase.

The conclusion that patterns of torque application do not change with fatigue is consistent with measurements taken by Beelen et al. (1995). Beelen et al. studied able-bodied individuals cycling an isokinetic ergometer using NMES induced contractions of the right quadriceps muscles. Peak pedal forces measured by Beelen et al. decreased by 30%, and the rate of force development declined proportionally to peak force ($r = 0.94$). Although time to

peak force was not directly measured, the proportional change in peak force and rate of force development suggests that timing would have remained relatively constant.

7.1.4 Summary

Over a period of 5 minutes continuous cycling, there was a reduction in power output by the quadriceps muscles of approximately 50%. There was little change, however, in the shape of crank torque curves resulting from this declining power output. When normalised to 100% peak torque, there was no apparent difference between trials collected when the muscles were fresh and when the muscle had fatigued.

The assumption of constant shaped torque patterns as the muscles fatigue will be important for subsequent sections of this thesis. Model parameters will need to be adjusted to account for changing force levels with fatigue. The current results suggest, however, that simply changing the maximum isometric force of the muscles is sufficient to model changes with fatigue. There is no need to alter the model's rate of torque rise or fall to maintain a match between measured and modelled torques.

7.2 NMES firing angles to maximise power output by the quadriceps muscles

7.2.1 Introduction

The modelling process originally began with the expectation that responses to NMES would vary between SCI individuals, with quite different optimum stimulation patterns for each subject. It was anticipated that modelling kinematic patterns for each subject would enable prediction of the optimum pattern for those subjects. Figure 7.2.1.1, however, illustrates that the measured responses were relatively similar for the cohort of subjects examined. Furthermore, simulated torque curves also followed very similar patterns for all subjects (Figure 7.2.1.2). Therefore, average curves will be used for the majority of comparisons

between measured and modelled results, with curves for individuals being reported only when necessary.

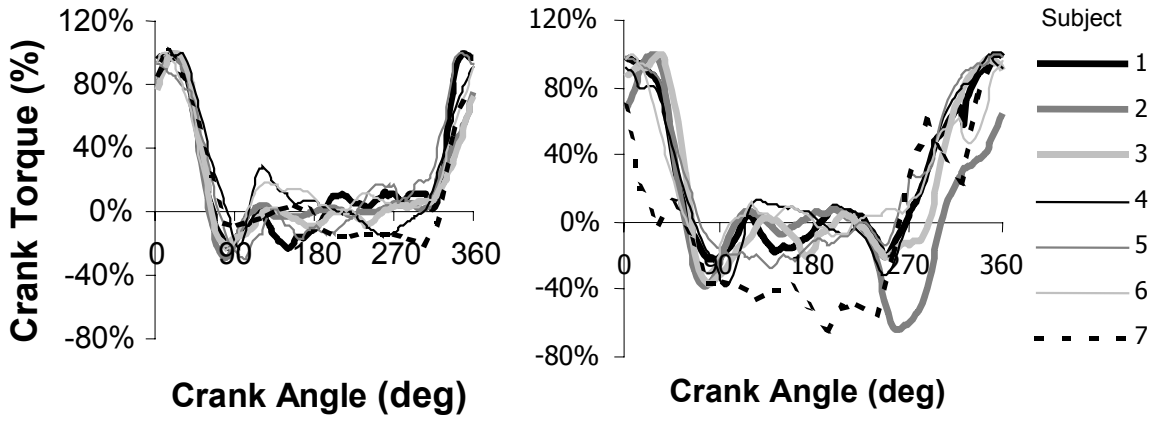

300 - 20 deg 220 - 20 deg

Figure 7.2.1.1 Individual crank torque curves for selected NMES firing angles of the quadriceps.

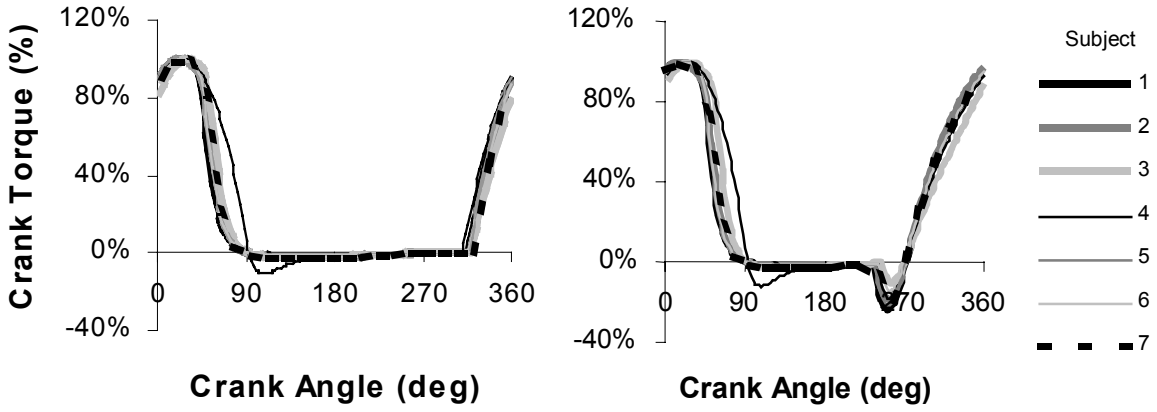

300 - 20 deg 220 - 20 deg

Figure 7.2.1.2 Modelled crank torques for the same trials shown in Figure 7.2.1.1. Note: Subject 4 had stimulation lasting until 60 deg, rather than 20. This is why the modelled torque decline looks different to the other subjects.

The torque pattern from one subject stands out in Figure 7.2.1.1b as being quite different to the others. This subject (7) used passive measurements taken from before the first active trial and it appears the subject moved in the chair resulting in changes to the passive torque levels. Consequently, nett measurements for this subject became less accurate as time progressed (see Section 7.1.3). As explained in Section 4.4.3, steps were taken to prevent this happening to subsequent measures for other subjects. The results from Subject 7 have therefore been excluded from all graphs of average pedal forces and torques as well as from calculations of power output. Correlation measures for this subject have been retained in order not to artificially inflate the match between measured and modelled results.

7.2.2 Comparison of modelled to measured results.

General description of pedal force and torque data.

During the angle seeking experiments, each subject was tested using a different sequence of stimulation firing angles in order to search for the angles that generated maximum average power output. For ease of data presentation, however, only a select range of angles will be illustrated in this section. The range of angles presented has been chosen to best represent apparent trends in the data as well as to maximise the number of subjects tested at each chosen angle.

It can be seen from Figures 7.2.2.1 and 7.2.2.2 that the model tracked the rise of crank torque very closely to the mean measured result for a range of stimulation onset angles. The decline in torque after stimulation ceased was not so well matched, hence this will be investigated in detail.

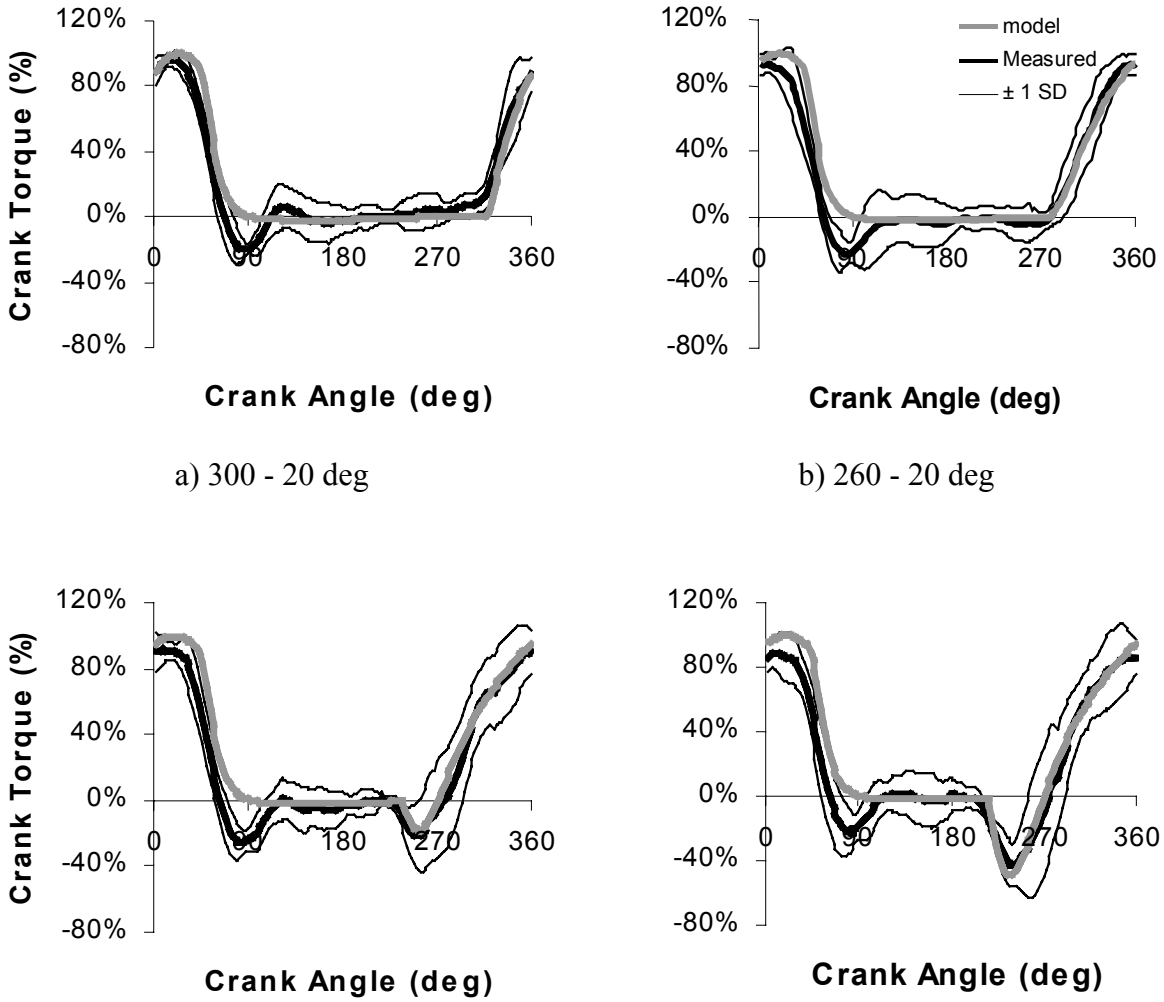

a) 300 - 20 deg

b) 260 - 20 deg

c) 220 - 20 deg

d) 200 - 20 deg

Figure 7.2.2.1 Average modelled and measured crank torque curves at selected angles of quadriceps stimulation onset.

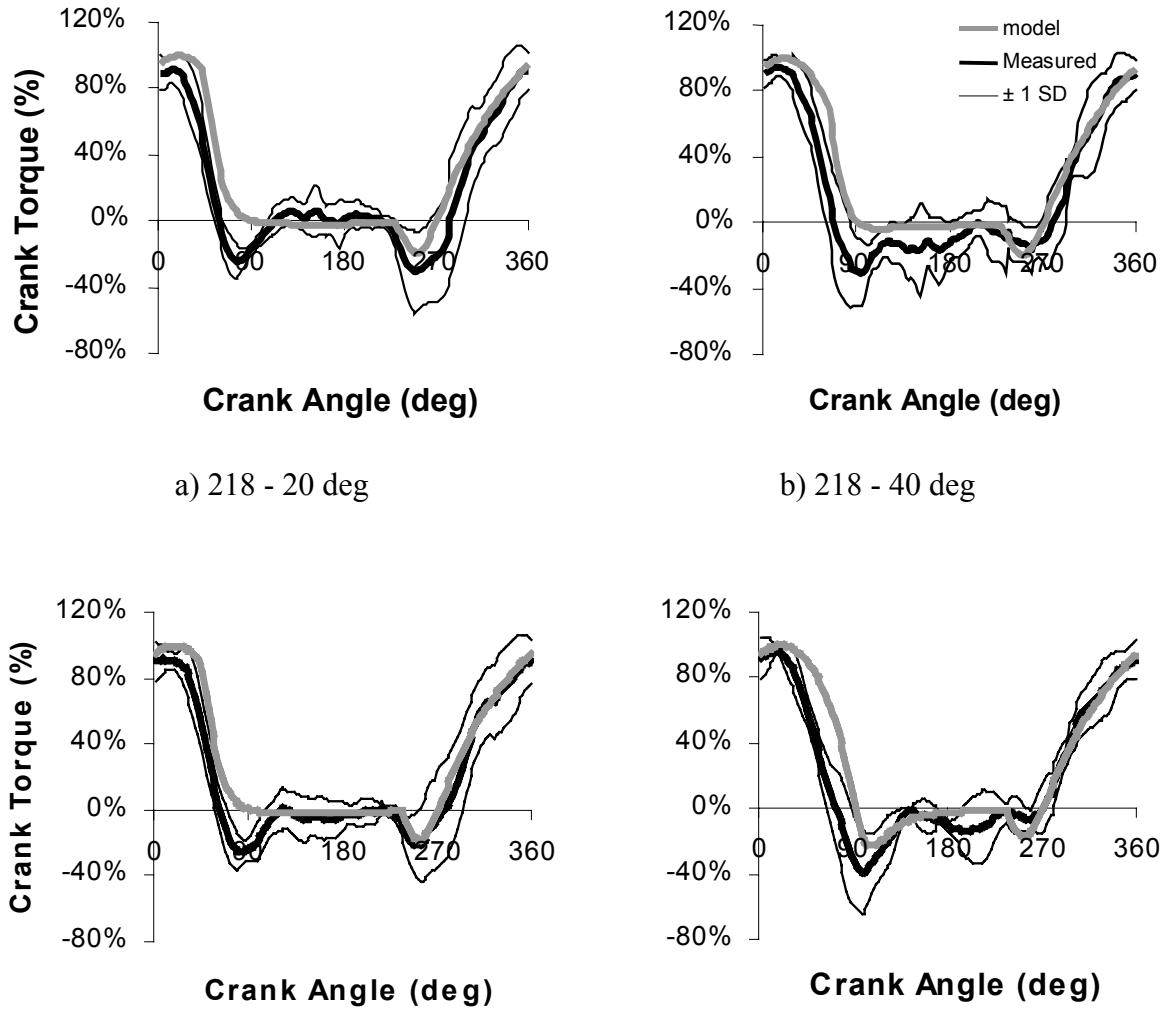

a) 218 - 20 deg

b) 218 - 40 deg

c) 218 - 60 deg

d) 218 - 70 deg

Figure 7.2.2.2 Average modelled and measured crank torque curves at selected angles of quadriceps stimulation cessation.

The measured crank torque peaked at crank angles of 14, 16, 22 and 18 deg for the four stimulation angles illustrated in Figure 7.2.2.2. Modelled torque peaked at 22 deg for all stimulation cessation angles with stimulation cessation angle having little effect on the angle of maximum torque production. This was because crank torque was already declining when stimulation ceased. The angle of peak torque occurred where the combination of knee extensor torque and the effectiveness with which knee extensor torque could apply torque to the crank was maximised. Figure 7.2.2.3 indicates that modelled knee extensor torque continued to rise after stimulation ceased because of the rise delay constant. The declining

crank torque after 20 deg must therefore have resulted from a less effective transference of knee extensor torque to crank torque after the angle of peak crank torque at 22 deg.

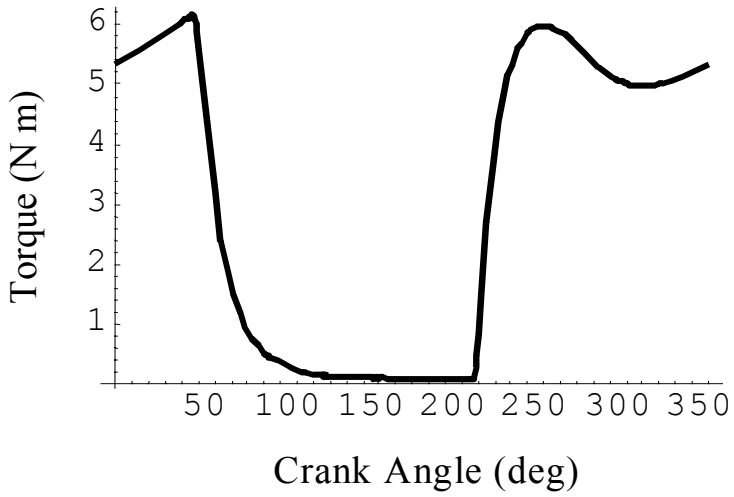

Figure 7.2.2.3 Modelled knee extensor torque for one subject with stimulation firing angles between 200 and 20 deg.

While the measured rise phase and angle of maximum torque was matched closely by the modelled crank torque curves, the measured torque declined rapidly after peak torque was reached. Modelling predicted the torque would remain high for longer, so that the modelled torque fell outside one standard deviation of the measured values during the declining phase for every angle investigated. Not only did measured torque decline rapidly, but there was an overshoot where torque became negative at the end of each muscle contraction. This negative period was expected for angles where stimulation was maintained too long (eg Figure 7.2.2.2 d), but occurred for all cessation angles. It can be seen from Figure 7.2.2.2 that the overshoot became larger for later cessation angles, but this effect was not great. The overshoot happened at all angles for every subject, to a greater or lesser extent, and made visual identification of optimum stimulation cessation angles very difficult during the data collection sessions (see Section 4.4.3).

A number of steps were taken to identifying the source of the rapid torque decline and subsequent overshoot. It was important to determine whether the differences were the result

of model error, measurement error, or some factor in the ergometer set up that violated the model's assumptions.

It was considered possible that the measured torque was being affected by changes in crank angular velocity. The ergometer's motor was supposed to maintain constant velocity cycling throughout each revolution. Even with no active muscle contractions, however, there was a change in velocity of approximately plus or minus 5% from the average value. Figure 7.2.2.4 illustrates typical mid-revolution changes in velocity for both active and passive cycling by one subject. Active cycling, although changing the pattern of velocity fluctuations, did not alter the overall range of velocities measured. It seemed likely that changes in velocity during active cycling may have generated inertial forces on the crank that differed from passive conditions. Inertial parameters were excluded from the model on the assumption that cycling was isokinetic. Perhaps the violation of this assumption was affecting the model's ability to predict torque patterns.

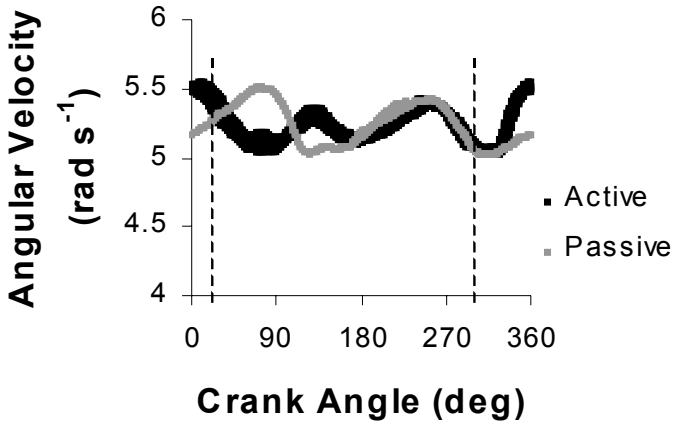

Figure 7.2.2.4 Crank angular velocity - angle curves for one representative subject during active and passive cycling. Vertical dotted lines represent the stimulation onset and cessation angles of 300 and 20 deg respectively.

While violation of the constant velocity assumption clearly must have affected measured torque values, the magnitude and direction of expected changes did not match the differences between measured and modelled torques. During the first 90 deg after TDC, the active crank

velocity was slowing while, during passive cycling, the velocity was increasing (Figure 7.2.2.4). If the ergometer motor was slowing the cranks then this would have been expected to increase force applied to the crank while momentum from the legs was being absorbed. The measured crank torque was less than that predicted by the model however, suggesting that something other than simple slowing of the crank was responsible. One possibility was that the velocity of rotation affected pedal forces directly through centripetal effects as well as indirectly through acceleration.

In order to investigate velocity effects more thoroughly, the model was modified slightly to include measured velocity changes and estimates of the leg inertial parameters. Thigh and shank masses were set at 6.5 and 3 kg respectively. While these may have been over-estimations of segment mass, this decision was taken in order to exaggerate any inertial effect. Crank torque was predicted by the model using these segment masses, assuming no active muscle forces and using the velocity fluctuations during both active and passive cycling from Figure 7.2.2.4.

Figure 7.2.2.5 illustrates an estimation of error calculated by subtracting the crank torque predicted using the passive velocity fluctuations from the torque predicted using the velocity fluctuations measured during active cycling. As suggested above, Figure 7.2.2.5 shows that the changes in velocity would be expected to increase crank torque for angles in the first quadrant after TDC. Figures 7.2.2.1 and 7.2.2.2, however, show that the model is overestimating crank torque through this range. Furthermore, even with deliberately overestimating segmental masses, the anticipated error was relatively small when compared with the large overshoot in measured torque following stimulation cessation. Therefore, the model's error is unlikely to have resulted only from the constant velocity assumption, and some other explanation must be sought to explain the difference.

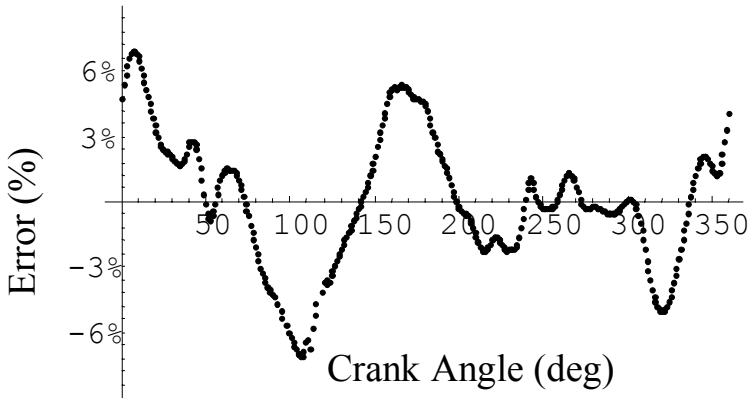

Figure 7.2.2.5 Predicted error in modelled crank torque resulting from changes in crank velocity with muscle activation. Torque differences have been expressed as a percentage of peak measured torque for ease of comparison with Figure 7.2.2.2. See text for details.

Vertical and horizontal forces applied to the pedal for a single subject using stimulation firing angles between 300 and 20 deg are shown in Figure 7.2.2.6. Consideration to the general shape of these curves will be given later, however considering the patterns in these graphs during the period after stimulation ceases will advance the present discussion. Both vertical and horizontal forces in Figure 7.2.2.6 demonstrate oscillations in force level during the expected passive phase of the revolution between 90 and 320 deg. Most subjects repeated this oscillatory pattern after stimulation cessation, although magnitudes differed considerably. Figure 7.2.2.7 illustrates these curves averaged across all subjects for these firing angles. While individual subjects differed in responses, the oscillations are still obvious from Figure 7.2.2.7; particularly in the vertical direction.

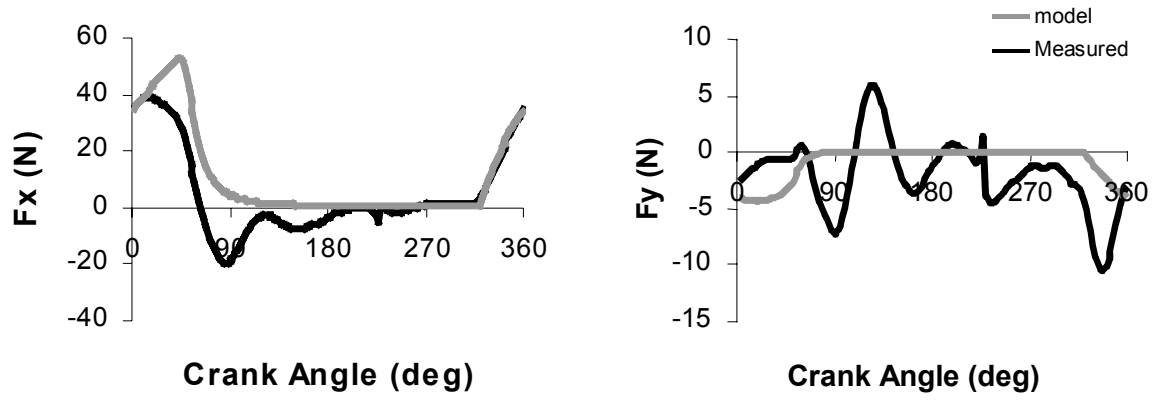

Figure 7.2.2.6 Horizontal and vertical pedal forces measured for Subject 6 with stimulation firing angles between 300 and 20 deg. Positive forces are defined as acting forward and down on the pedal, as illustrated on Figure 4.4.4.1.

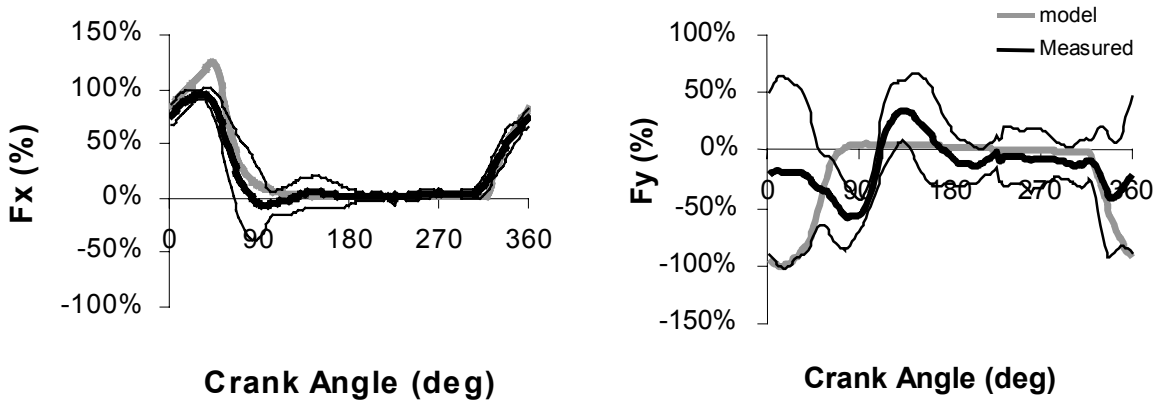

Figure 7.2.2.7 Horizontal and vertical pedal forces measured for all subjects with stimulation firing angles between 300 and 20 deg. Modelled forces were normalised against their respective maximum measured forces.

These damped oscillations suggest storage of elastic strain energy during the muscle contraction and subsequent release after stimulation cessation. The most likely location for this elastic effect is in a rubber drive belt connecting the ergometer's cranks to the resistive motor. Figure 7.2.2.8 illustrates that, as force was applied to the pedal, this would have stretched the lower half of the drive belt. When crank torque started to decline after the peak

around 20 deg, the elastic belt would have relaxed, loosening tension in the belt and thus decreasing the force applied to the pedal. The negative overshoot at the bottom of the torque-angle curve and subsequent oscillatory patterns may be the result of the belt rebounding during the passive phase of cycling. The earlier than expected decline in measured torque can also be explained by this hypothesis as the belt starts to relax following peak torque.

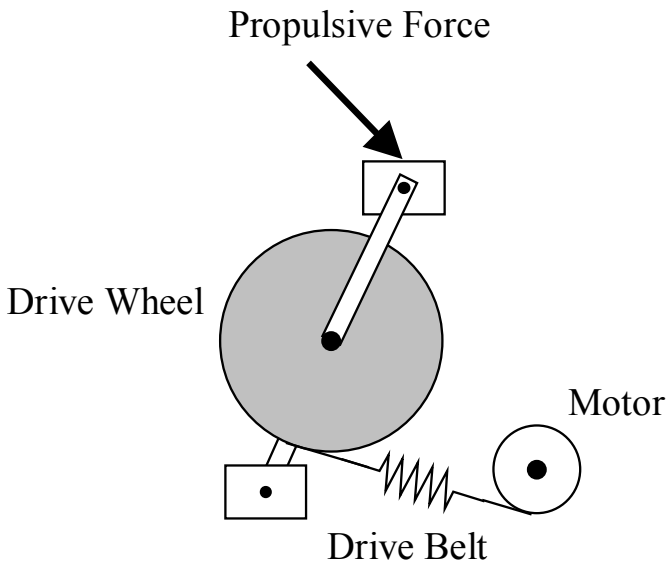

Figure 7.2.2.8 The ergometer's drive system illustrating the elastic nature of the drive belt connecting the cranks to the motor.

The rapid torque decline and subsequent overshoot could also be explained by an inadequate response by the motor controller. As torque rose after stimulation commenced, the crank velocity increased and thus the controller would have drawn increasing levels of current from the motor in order to resist further acceleration. When torque began to decline after 20 deg, crank velocity slowed and thus the controller would have reduced current to the motor to prevent velocity dropping too far. A delay in motor response may have caused the controller to reduce current more than was necessary to match torque, in order to prevent further slowing of the crank. If the motor was providing too little resistance, this could have resulted in the rapid decline in torque and subsequent overshoot. The subsequent oscillations during passive cycling could indicate the controllers attempt to stabilise velocity. Perhaps any

elasticity in the ergometer drive system would have exaggerated these oscillations making predictions by the motor control system more difficult.

Further comparisons between measured and modelled data will therefore concentrate on the rise of crank torque, this portion being less affected by the ergometer control system. Correlations between measured and modelled data will still be made on whole crank revolutions, however it will be understood that much of the mismatch will have resulted from the declining portion of the torque curve.

Vertical forces applied to the pedal were generally small and did not contribute greatly to propulsion. Modelled vertical pedal forces were always negative (lifting pedal up), however the vertical forces measured were quite variable (Figure 7.2.2.7 b). Some subjects produced negative vertical forces of greater magnitude than those predicted by the model (eg Figure 7.2.2.9 a) while others produced vertical force in a different direction to that predicted by the model (eg Figure 7.2.2.9 b). Because the hip and pedal were at a similar horizontal alignment around TDC, extending the knee would push the pedal almost directly forward. Therefore, only small changes in modelled vertical hip position were required to change direction of the small vertical force. Sensitivity analysis reveals that changing the modelled hip height will markedly affect the resulting modelled vertical pedal forces with only minor effect on horizontal force and hence crank torque (Figure 7.2.2.10).

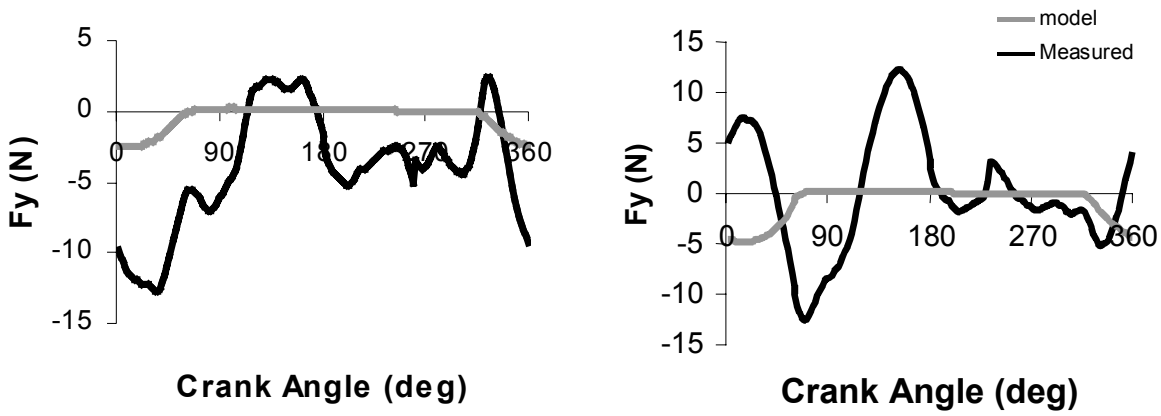

a) Subject 1

b) Subject 3

Figure 7.2.2.9 Example vertical force patterns for two subjects with stimulation firing angles of 300 to 20 deg

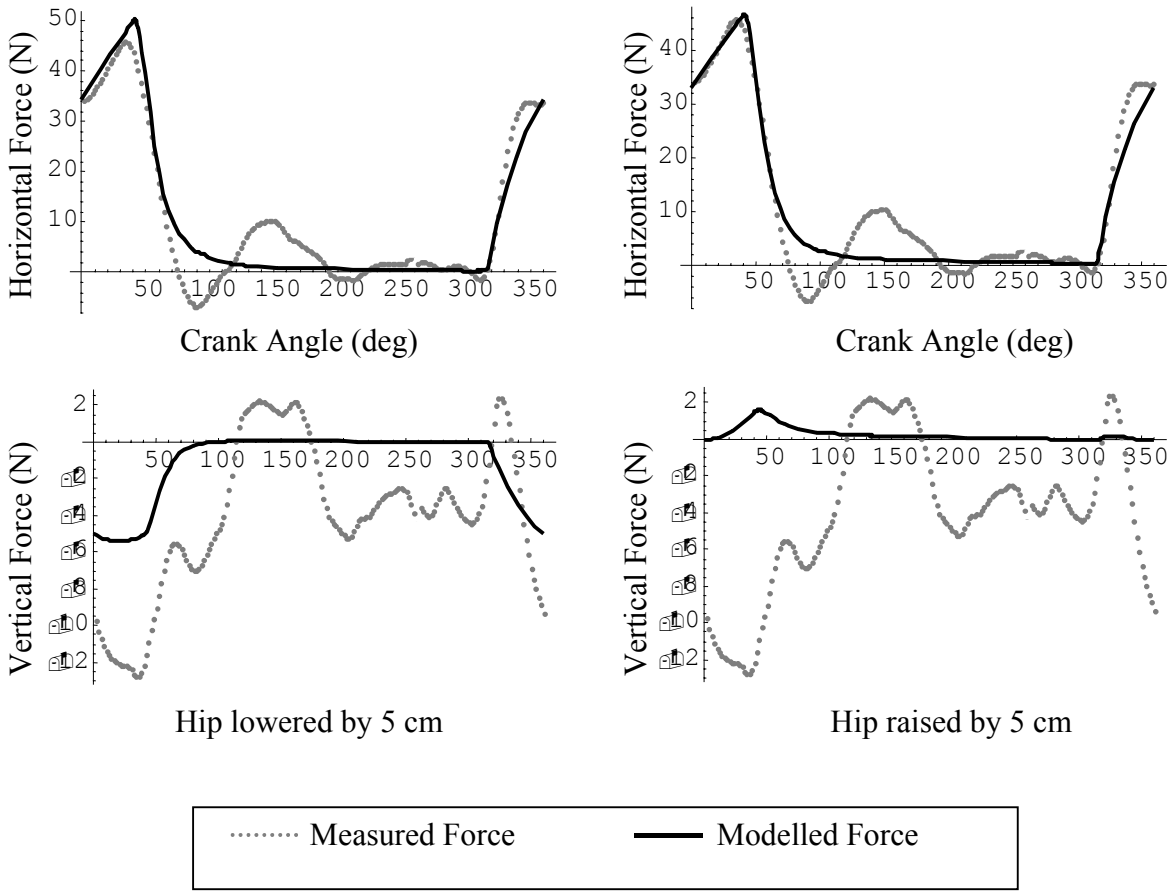

Figure 7.2.2.10 The effect on modelled pedal forces from changing modelled hip height by 5 cm in one representative trial.

When identifying the location of the greater trochanter, able-bodied subjects would usually be asked to stand and move their hips from side to side, so that movement of the trochanter could be felt with respect to the acetabular rim. The inability to perform this procedure with SCI subjects, together with their tendency to accumulate adipose tissue over the hips, reduced the accuracy with which hip markers were positioned. Furthermore, Neptune and Hull (1995) have shown that the greater trochanter may misrepresent the hip centre by up to 3.5 cm in the vertical direction. Therefore, an error of at least 5cm in vertical hip displacement was not unexpected. Fortunately, around TDC where the quadriceps muscles are most active, vertical forces make little contribution towards crank torque and therefore the model's primary output is relatively insensitive to this inaccuracy.

Horizontal forces provide most of the crank torque because they are larger in magnitude than vertical forces, and because they are most active around TDC when horizontal forces best serve to apply torque to the crank (Figure 7.2.2.6). The major features of the horizontal force curves have therefore already been described with respect to crank torques. That is, the modelled rise in horizontal force matches measured data quite well, however the modelled force continues to rise after the measured force has begun to decline (Figure 7.2.2.11). While the measured horizontal forces did not continue to rise until the muscle relaxed as the model predicted, the forces did not rapidly decline in a manner expected if the stimulation had ceased early. Figure 7.2.2.11 appears to show both measured and modelled force curves being switched off at the same crank angles. Therefore, the effect we are seeing is a failure of the measured force to rise as much as predicted, not an error in the timing of stimulation. The plateauing of measured force is consistent with a reduction in resistance; caused either by inadequate motor control and/or an elastic effect in the ergometer drive belt.

There was a pronounced “dip” during the rise of horizontal pedal force for those trials with advanced stimulation firing angles (Figure 7.2.2.11). This dip was present in the both measured and modelled data, although it was more pronounced in the measured data. The knee reached maximum flexion at approximately 270 deg and extended thereafter. Trials with significant quadriceps muscle force before 270 deg would therefore be initially producing eccentric contractions of these muscles. The knee extended after 270 deg, thus shortening the quadriceps towards their optimum fibre length and increasing the moment arm of the quadriceps at the knee. Both these effects would be expected to increase the force of the quadriceps. At the same time, increasing velocity of muscle shortening would tend to reduce the muscles’ force. These two effects would have interacted to produce a dip in the knee extension torque (Figure 7.2.2.3) as the velocity and the length/moment arm effects switched dominance. The pedal force patterns from Figure 7.2.2.11 would have resulted from these changes in knee extension torque.

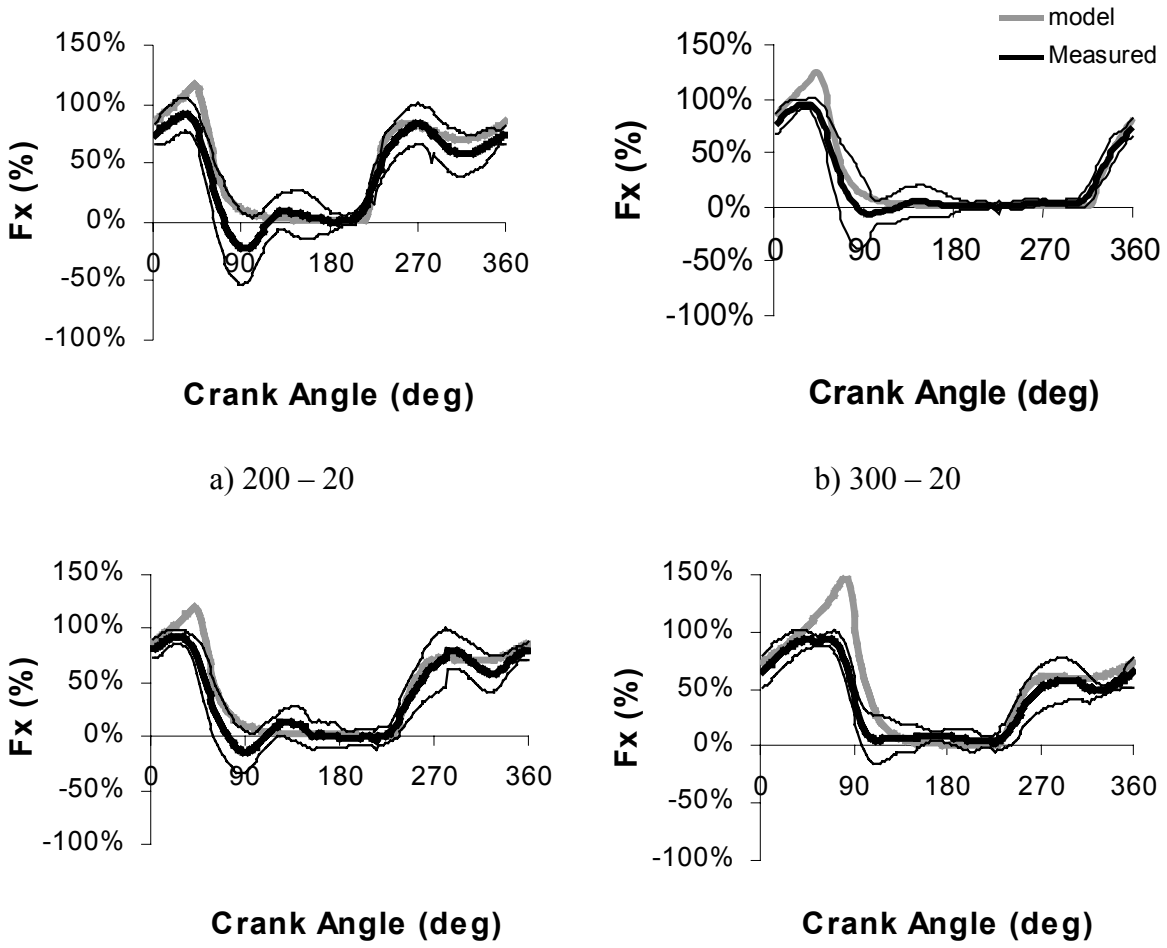

a) 200 – 20

b) 300 – 20

c) 218 – 20

d) 218 - 60 deg

Figure 7.2.2.11 Measured and modelled horizontal pedal forces at selected stimulation firing angles.

7.2.3 Effect of changing stimulation onset angle

Changes in crank torque with stimulation onset angle

Stimulation after an angle of approximately 270 deg always generated positive torques on the cycle crank (Figure 7.2.2.1). If the quadriceps developed force before this angle, a period of negative crank torque was generated that retarded propulsion (Figure 7.2.2.1 c, d). Once stimulation was early enough to generate a negative component, further advance of stimulation onset increased the size of the negative component, but did not change the angle where torque changed over from negative to positive. If the quadriceps did not develop force until after 270 deg (eg Figure 7.2.2.1a) there was no negative torque developed; however the area underneath the positive torque was less than when stimulation commenced earlier.

The simulated crank torques were, on average, able to predict both the timing and magnitude of negative torque components resulting from early stimulation of the quadriceps. Individual measures of the angles where torque changed from negative to positive were not as precise as may be indicated by the average curves in Figure 7.2.2.1. This is likely to be because oscillations in the torque levels during the passive phase before stimulation commenced are likely to have exerted influence on the early components of torque rise. Differences between trials cancelled out so that the modelled torque matched average measured torques very closely up until the angle of peak torque.

Change in correlation between measured and predicted stimulation onset angles

Stimulation onset was examined at representative crank angles every 20 deg between 200 and 300 deg. Correlations were available for seven subjects at all angles except 300 deg, as only six subjects were tested experimentally at this angle. Correlations for all subjects and angles averaged 0.83 and varied between 0.48 and 0.95. A one-way ANOVA with repeated measures found no significant change in correlation with stimulation firing angle ($p=0.081$). As described above, passive levels for Subject 7 changed during the testing session resulting in progressively poorer correlations for this subject over time (Figure 7.2.3.1). Other subjects showed no consistent pattern of change; a finding supported by the ANOVA results. The lack of change in correlations between modelled and measured torques with stimulation firing angle suggests that modelled changes in crank torque were similar in trend to those measured experimentally.

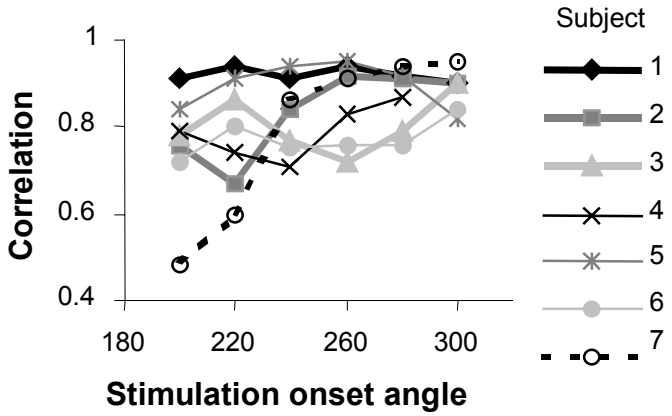

Figure 7.2.3.1 Changes in correlation between measured and modelled crank torques with stimulation onset angle.

Measurement of activation timing during the isometric knee extension experiments found that the time for muscles to generate torque in response to stimulation onset varied with knee angle. While this variation was statistically significant across knee angles between 15 and 90 deg, the amount of change was relatively small for the range of knee angles measured during the present cycling experiments. For this reason, activation timing constants were not adjusted for knee angle within the present model. The results from this section suggest that this simplification was justified, with no apparent variation in the model's ability to predict torque responses at each stimulation firing angle.

Measured Power Output

The period of negative torque applied to the crank when stimulation commenced too early would be expected to reduce average power output. Stimulation commencing too late would also reduce power because there would be reduced area under the torque-angle curve (Work = $\int T\, d\theta$). Therefore, an optimum firing angle was expected to exist that maximised power output while cycling. Figure 7.2.3.2 illustrates the average power output measures taken from four subjects plotted against stimulation commencement angle. The other subjects produced similar results but have been omitted from this figure for clarity of presentation. Results for all subjects may be found in Appendix 4.2.2. The arrows on Figure 7.2.3.2 illustrate the order of trials for each firing angle. While there appear to be quadratic trends for each subject, peaking between 230 to 250 deg, there is a clear sequence effect as well with the

first trials generating greater power output. Therefore, any attempt to calculate the peak firing angle had to consider the order of trials to account for progressive fatigue of the muscle.

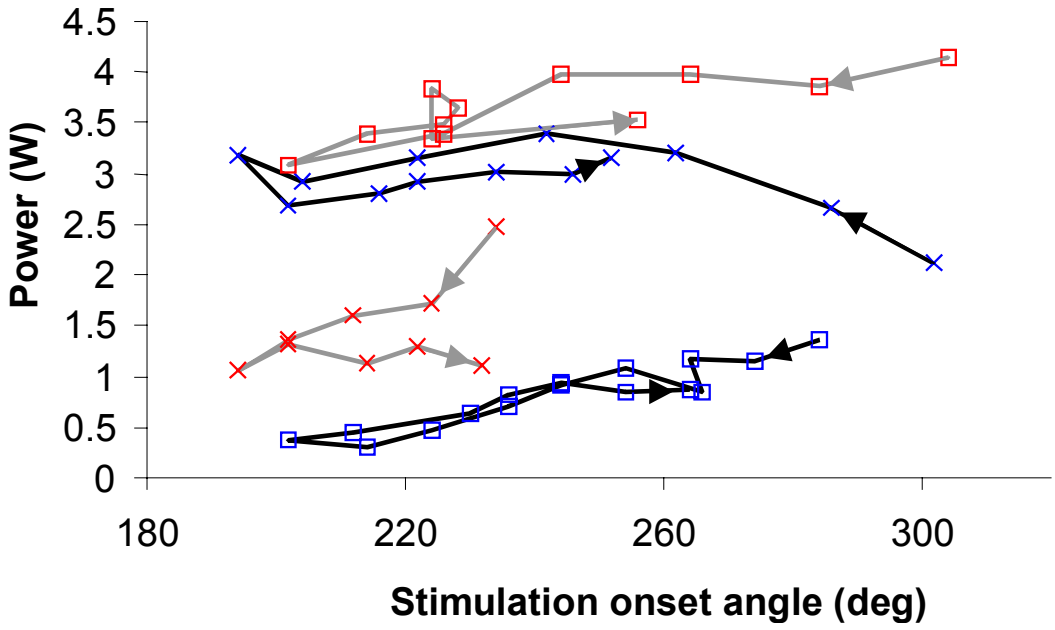

Figure 7.2.3.2 Change in power output with quadriceps NMES onset angle for four representative subjects. See text for details.

To calculate peak stimulation firing angle, a Non-Linear Analysis of Regression was performed using the following equation from Section 4.4.4:

$$\text{Power} = a \times \text{stimon} + b \times \text{stimon}^2 + c_i + e^{d_i \times \text{trial}}$$

Equation 7.2.3.1

The regression produced a high correlation between measured and predicted power ($R^2 = 0.94$), however, the standard errors for most parameters were rather high when considered as percentages of those parameters (Table 7.2.3.1). This reduces our confidence in the resulting values for these constants.

Table 7.2.3.1 Constants for Equation 7.2.3.1 from Analysis of Regression predicting power output from quadriceps stimulation onset angle.

			Asymptotic 95 % Confidence Interval	
Constant	Estimate	Asymptotic Std. Error	Lower	Upper
a	0.100	0.019	0.062	0.138
b	-0.00020	0.00004	-0.00027	-0.00012
c_1	-11.3	5.1	-21.4	-1.1
c_2	-11.9	2.3	-16.5	-7.2
c_3	-9.6	0.2	-10.1	-9.1
c_4	-9.8	2.3	-14.4	-5.1
c_5	-9.5	0.0	-9.5	-9.5
c_6	-9.0	1.0	-11.1	-6.9
d_1	-0.095	2.293	-4.679	4.489
d_2	-0.408	0.301	-1.009	0.193
d_3	-0.334	0.239	-0.812	0.144
d_4	-0.153	0.217	-0.587	0.282
d_5	-25.4	2.3	-30.0	-20.7
d_6	-0.381	2.272	-4.922	4.159

Section 4.4.4 demonstrates how constants a and b from Equation 7.2.3.1 can be used to calculate the stimulation angle giving peak power; and how the standard error of the estimate for those constants can then be used to estimate the uncertainty in peak angle. Applying Equations 4.4.4.4 to 4.4.4.6 to values from Table 7.2.3.1 gives a peak stimulation angle of 253.6 deg with uncertainty due to constants a and b of 50.9 and 53.3 deg respectively. That is, the peak angle can only be confidently located somewhere between 200 and 307 deg.

Although the above calculations using standard error of the estimate give a high level of uncertainty, using the 95% confidence intervals from Table 7.2.3.1 would have given an even greater range of possible peak angles. For example, the 95% confidence intervals for constant a were 0.062 to 0.138. If half this range of intervals (0.076) had been used as the measure of uncertainty in equation 4.4.4.5, the estimated uncertainty would have been nearly four times that found when the standard error of the estimate was used. Visual inspection of Figure 7.2.3.2 suggests that the standard error of the estimate provides a more realistic estimate of the range in possible peak stimulation onset angles from uncertainty in the regression constants.

The relatively flat curves represented in Figure 7.2.3.2, combined with inconsistent fatigue characteristics, make it difficult to improve upon this level of uncertainty. While Figure 7.2.3.2 suggests that there may be a slightly different optimum angle for each subject, applying regression analyses to individual subjects was tried and resulted in much larger uncertainties in peak angle for each individual, owing to the reduced number of data points available. It appears that, within this range of angles, cycling power output is not particularly sensitive to quadriceps firing angle for the cohort of subjects examined.

Prediction of peak stimulation firing angle from computer simulations.

Stimulation firing angle affects the amount of work performed by the muscles. Figure 7.2.3.3 illustrates the effect of advancing stimulation firing angle from 300 to 200 deg. Work done on the crank can be seen from this figure as area under the torque-angle curve. Work done per revolution is directly proportional to power output when angular velocity is kept constant. Advancing the firing angle from 300 to 240 deg increased total work by enlarging the positive area under the curve. Firing angles in advance of 240 deg increased the negative area with little effect on positive propulsion. It can be seen from Figure 7.2.3.3 that the changes predicted by the model track those measured directly. Figure 7.2.3.3 b suggests that the peak stimulation firing angle was likely to be near 240 deg.

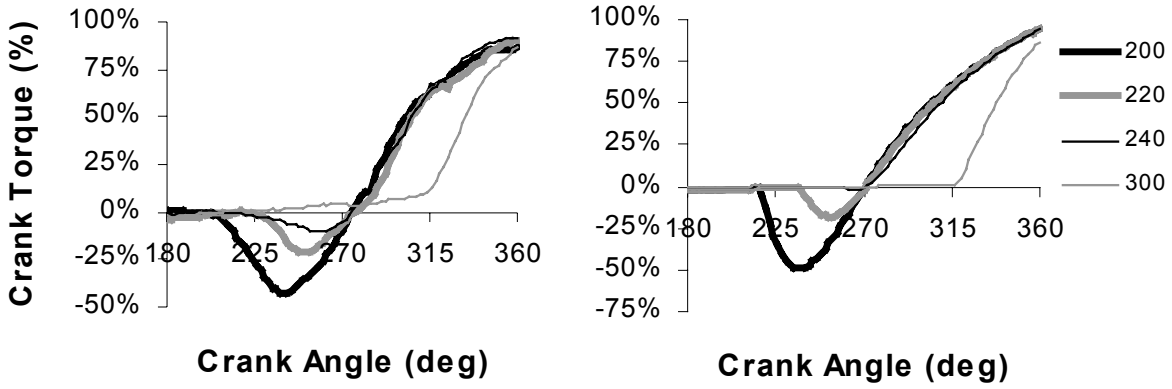

a) Measured crank torques b) Modelled crank torques

Figure 7.2.3.3 Measured and modelled rises in crank torque with different NMES onset angles. The number for each trial represents the crank angle at which quadriceps stimulation commenced.

In order to predict the peak firing angle more precisely, an optimising routine was performed to find the stimulation firing angles that maximised work done. This was a simple procedure that iteratively changed the model's stimulation onset angle and measured the work done per revolution using each onset angle. The stimulation onset angle generating the greatest work was identified to the nearest 0.01 radian. The average stimulation onset angle predicted by these simulations was 236.4 deg, with no subjects differing by more than 3.2 deg from this average value. This was 17.8 deg in advance of the measured angle of peak power (253.6 deg), but well within the measurement uncertainty of plus or minus 50 deg. Although the model appears to accurately predict measured responses to stimulation onset (Figure 7.2.3.3), the large uncertainty in measured angle of peak power makes it difficult to confirm this with confidence at present. Results from measurements of stimulation cessation angles have a bearing on stimulation onset and hence will be detailed in the following section before the accuracy of model predictions is discussed further.

Figure 7.2.3.4 compares the change in power output with stimulation onset angle predicted by the model with values calculated from measured data by applying constants from Table 7.2.3.1 to Equation 7.2.3.1. The measured data suggest that delaying quadriceps NMES onset angle by 20 or 40 deg from peak would decrease power output by respectively 4.6 and 15.6 %. The model gives comparable values of 3.7 and 11.7 %.

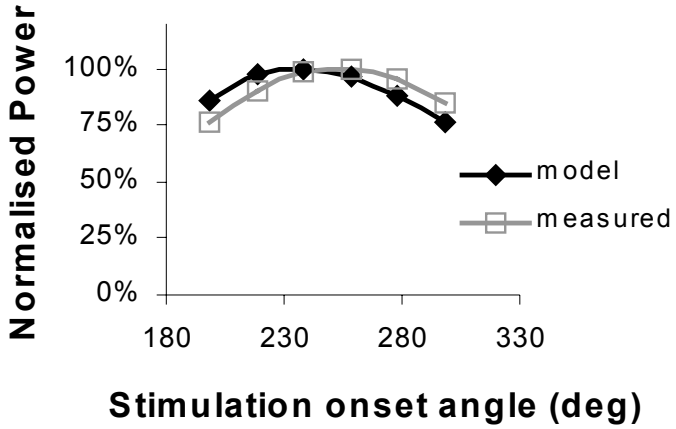

Figure 7.2.3.4 The effect of quadriceps stimulation onset angle on power output.

7.2.4 Effect of changing stimulation cessation angle

Changes in crank torque with stimulation cessation angle

Changing the stimulation cessation angle did not affect the crank torque curve as much as was initially expected. The reason for this can be seen by viewing Figure 7.2.4.1. The measured and modelled curves are quite similar in Figure 7.2.4.1, however the following explanation is easier to follow from the modelled curves in Figure 7.2.4.1 b. When stimulation was maintained until 70 deg, the torque applied to the crank declined after its peak at approximately 20 deg as the crank angle changed, and subsequently altered the effective moment arm of the applied horizontal pedal force. After about 90 deg, contraction of the quadriceps generated negative torque on the crank. It can be seen from Figure 7.2.4.1 that, when stimulation ceased earlier, the crank torque began to drop more quickly, however the effect was not substantial because torque was dropping away from an already declining curve.

If the quadriceps were active after 90 deg or ceased activity before 20 deg, these would have had more effect on work done on the crank. Between these angles however, the change in area under the curves was not substantial. This will be likely to affect the precision in determining stimulation angles that maximised average power output in the following section.

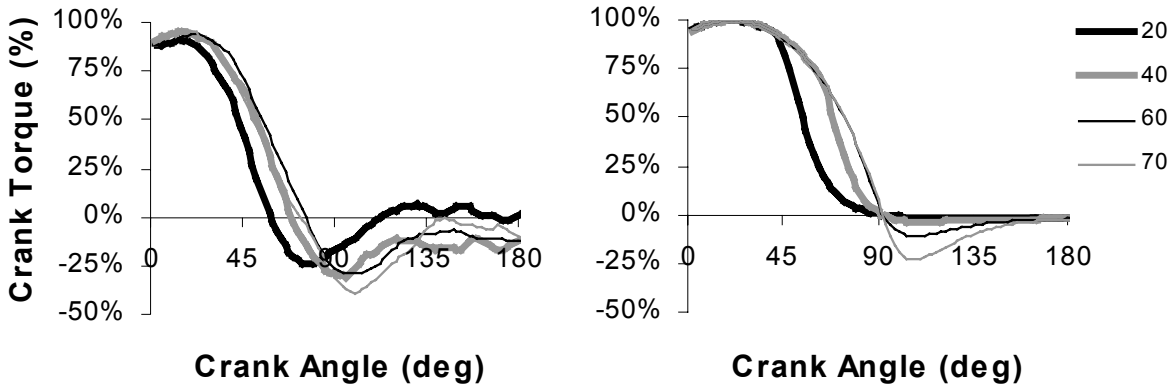

a) Measured crank torques b) Modelled crank torques

Figure 7.2.4.1 The effect of changing stimulation cessation angle on measured and modelled crank torques. The number for each trial represents the crank angle at which quadriceps stimulation ceased.

Correlation change with angles of stimulation cessation

Correlations for stimulation cessation angles were tested at crank angles every 10 deg between 20 and 70 deg. Again, because different sequences of angles were tested for each subject, not all subjects completed trials at all of these representative angles. Correlations were available for five subjects at 70 deg, six subjects at 20 and 50 deg and all seven subjects at the other angles. Correlations for all subjects and angles averaged 0.77 and varied between 0.34 and 0.97.

The model tracked changes in stimulation cessation angle with no apparent change in correlations Figure 7.2.4.2. As with stimulation onset, the one subject generating very poor correlations was number 7, the subject with passive levels varying between successive trials.

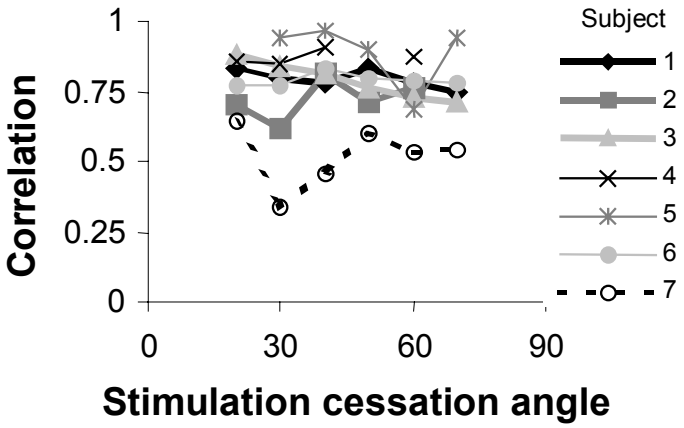

Figure 7.2.4.2 Changes in correlation between measured and modelled crank torques with stimulation cessation angle.

Measured Power Output

The change in average power output with stimulation cessation angle is illustrated by Figure 7.2.4.3. As for stimulation onset, there was a quadratic trend to these power/angle curves with an overlying sequence effect generated by progressive fatigue. The analysis of regression for these curves is provided in Table 7.2.4.1.

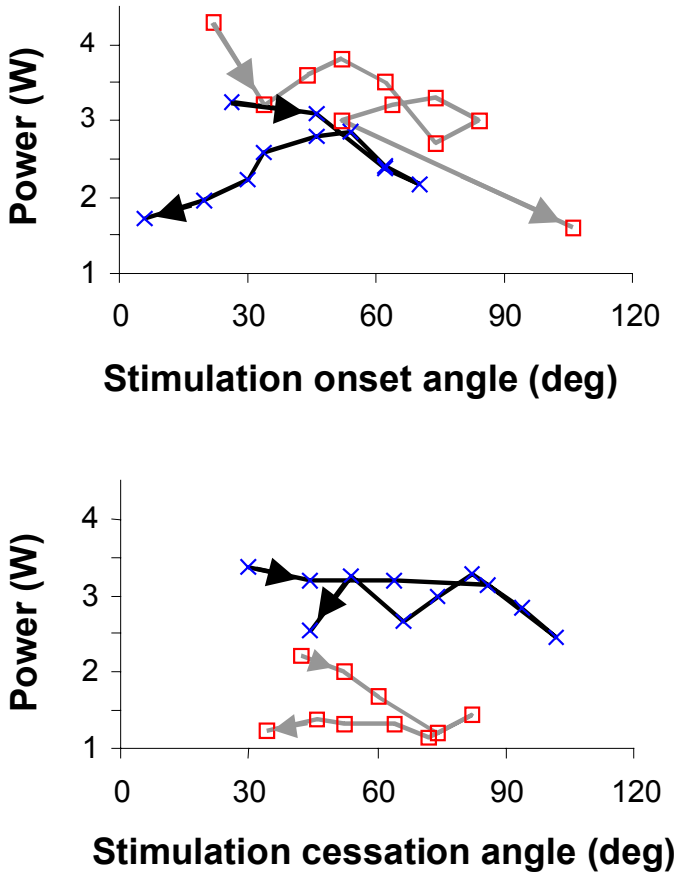

Figure 7.2.4.3 Change in power output with quadriceps NMES cessation angle for four representative subjects.

Table 7.2.4.1 Constants for Equation 7.2.3.1 from Analysis of Regression predicting power output from quadriceps stimulation cessation angle.

			Asymptotic 95 % Confidence Interval	
Constant	Estimate	Asymptotic Std. Error	Lower	Upper
a	0.031	0.011	0.010	0.052
b	-0.00032	0.00008	-0.00049	-0.00015
c_1	2.09	0.46	1.16	3.02
c_2	0.54	0.51	-0.50	1.57
c_3	1.67	0.28	1.12	2.23
c_5	1.80	0.41	0.97	2.63
c_6	2.31	0.55	1.21	3.42
d_1	-0.406	0.686	-1.788	0.976
d_2	-0.294	0.483	-1.268	0.679
d_3	-0.395	0.471	-1.343	0.554
d_5	-0.069	0.081	-0.233	0.095
d_6	-0.228	0.417	-1.068	0.612

Applying Equations 4.4.4.4 to 4.4.4.6 to values from Table 7.2.4.1 gives a peak stimulation cessation angle of 49.2 deg, with uncertainty calculated from the standard error of the estimate for constants a and b being 16.7 and 13.0 deg respectively. The precision with which peak cessation angle was determined belies the prediction made on page 228 that the angle giving maximum power would be difficult to isolate. The uncertainty in calculating peak cessation angle is considerably less than the comparative value for stimulation onset, where the angle could only be calculated with an uncertainty of 50 deg for each constant. The most likely reason for this is that, although the change in power output at angles near the peak may

not have been great, the changes at more extreme angles were enough to clearly define the shape of the quadratic curve for subsequent identification of the maximum.

Prediction of peak stimulation firing angle from computer simulations.

The model's optimising routine found the average angle of stimulation cessation that maximised work was 53.2 deg with all subjects being within 2.5 deg of this angle. This modelled angle was only 4 deg different to the measured angle generated peak power. Such a close fit between measured and modelled peak angle provides good support for the model's ability to predict stimulation firing angles. Even though control issues within the ergometer design limited the goodness of fit between measured and modelled torque curves during the declining phase, this did not hamper the model's ability to predict work done during this phase. It appears that the differences between measured and modelled torques remained relatively constant across stimulation cessation angles so that both resulted in the same maximum value.

The model predicted peak onset and cessation angles that were almost 180 deg out of phase (236.4 to 53.2 deg). This was initially surprising given the range of firing angles used by the commercially available Ergys ergometer was only 75 deg (Ergys Service Manual). With the benefit of hindsight, however, a range of 180 deg should have been expected. With a circular cycling action, the knee spends exactly half its revolution extending and the other half flexing. As long as the knee is extending, the quadriceps will be able to perform positive work and hence will contribute to propulsion. Only when a muscle performs negative work can there be energy absorbed from the pedals. The model predicted a range of firing angles of 177 deg rather than 180 deg because the modelled time for the muscle to develop force was slightly different to the relaxation time after stimulation ceased.

The peak stimulation firing angles measured experimentally from average power outputs were 253.6 to 49.2, a range of only 155.6 deg. The uncertainty in measuring stimulation onset angle, however, was much greater than the uncertainty in measuring cessation angle (approximately 50 and 16 deg respectively). Furthermore, the cessation angle predicted by the model was 53.2 deg, in close agreement to the measured angle. These factors mean that we have more confidence in the measured peak cessation angle than we do in the angle of stimulation onset. If 180 deg is added to the measured cessation angle we get 229.2, much closer to the modelled peak angle of 236.4 deg. This suggests that the difference between

measured and modelled peak stimulation angle may well be a function of uncertainty in measurement, rather than model error.

Figure 7.2.4.4 compares the change in power output with stimulation onset angle predicted by the model with values calculated from measured data by applying constants from Table 7.2.4.1 to Equation 7.2.3.1. The measured data suggest that advancing the quadriceps NMES cessation angle by 20 or 40 deg from peak would decrease power output by respectively 6.3 and 20.2 %. The model gives comparable values of 4.8 and 20.5 %.

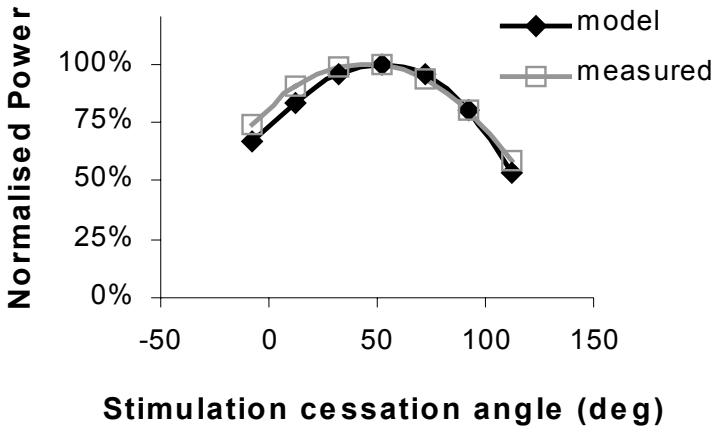

Figure 7.2.4.4 The effect of quadriceps stimulation cessation angle on power output

7.2.5 Summary

It appears that the model performed quite well in predicting performance of the quadriceps muscles. The model accurately predicted the patterns of torque rise in response to stimulation, however there was significant mismatch between measured and modelled curves after torque peaked. This mismatch appears to result from an inability of the ergometer to exactly control the crank angular velocity rather than from an error within the model. This conclusion was reached because, even though the measured torque declined earlier than the model, the stimulation cessation angle measured to maximise average power output was very close to that predicted by the model.

The model predicted that power output would be maximised with quadriceps NMES applied between crank angles of 236 and 53 deg; a duty cycle of 177 deg. The peak firing angles measured experimentally were 254 to 49 deg, with uncertainties of 52 and 15 deg respectively. The nominal uncertainties in peak firing angles were high because the effects of random variation in power output and progressive fatigue were substantial compared with the amount of change in power output with firing angle. The ability of the model to predict variations in crank torque with NMES firing angles, however, increases confidence in the model's ability to accurately predict peak acute firing angles. There was little variation between subjects in the range of firing angles required to maximise power output of the quadriceps muscles. Sections 7.5 and 8.2 will discuss how these firing angles would be affected by the location of the ergometer seat with respect to the crank.

It should be emphasised that the effects of stimulation firing angles on power output being discussed are for an acute period of only 10 s cycling. The measured responses show general agreement to the model predictions for the current experiment and similar ranges of firing angles have previously been proposed by a model reported by Schutte et al. (1993) for the ERGYS ergometer. Experimental measures by Glaser et al. (1993), however, on the effect of widening stimulation firing angles over the duration of a training session have not supported the use of wider firing angles. This point will be taken up again in Section 8.5 where the physiological response to an extended period of cycling will be discussed.

If this experiment were to be repeated, it is recommended that a different protocol be used to identify peak stimulation firing angles. Given that all subjects produced similar results, it would have been better to use exactly the same range of firing angles for every subject. These could have been presented in random order to better partition out the fatigue effect, would have required fewer angles to be tested for each subject, and would have enabled a more rigorous statistical examination of the results. This statement is made, of course, with the benefit of hindsight. At the time of testing, it was believed that each subject would produce eccentric contractions at different ranges of angles, and it was considered important to avoid moving too far into the eccentric range. Even after a few subjects had been tested, it was still not possible to see that they were so similar because of the high measurement uncertainty. Only after testing and analysing all subjects did the similarities become apparent.

7.3 NMES firing angles to maximise power output by the hamstring muscles

7.3.1 Comparison of modelled to measured results.

Overview of crank torques produced by stimulation of the hamstring muscles.

There was considerable variation between subjects in response to stimulation of the hamstring muscles (Figure 7.3.1.1). Some of the variability in Figure 7.3.1.1 is associated with each subject having different angles for stimulation cessation. This effect however is relatively small. For example, crank torque for Subject 2 reaches a peak and then declines well before the other subjects in Figure 7.3.1.1. Torque levels for this subject always decline well in advance of stimulation cessation, indicating that stimulation timing is not responsible for the decline. By contrast, Subject 6 produces peak torque much later than Subject 2 and maintains torque near maximum levels until after stimulation ceases.

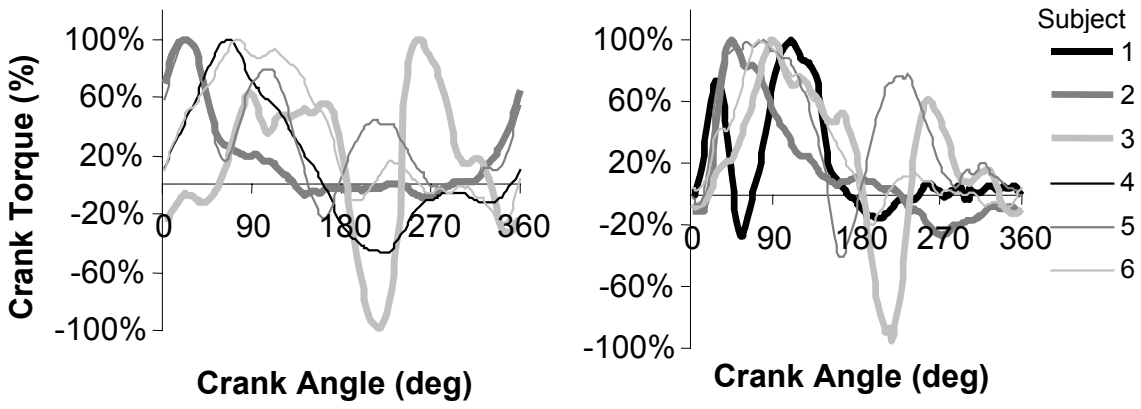

a) 300 degrees b) 360 degrees

Figure 7.3.1.1 Individual crank torque curves resulting from activation of the hamstring muscles at selected NMES onset angles.

The model does not predict this variability in the rise of crank torque in response to stimulation (Figure 7.2.1.2). It will be hypothesised below that some of the inter-subject variability may result from differences in hamstring moment arms between subjects.

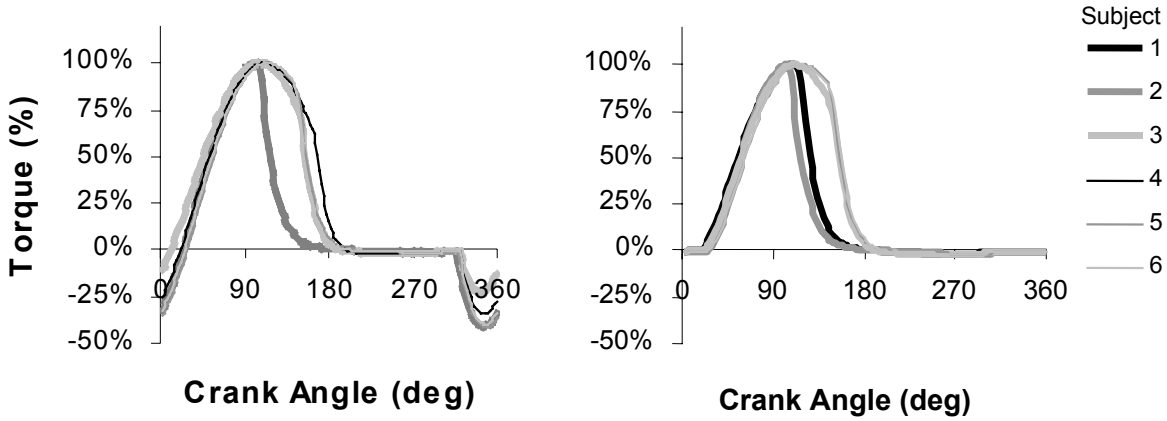

a) 300 degrees b) 360 degrees

Figure 7.3.1.2 Modelled crank torques for the same trials shown in Figure 7.3.1.1

Subject 7 produced strong contractions in response to hamstring stimulation that opposed propulsion of the ergometer. It appears likely that these were flexor withdrawal contractions, resulting from stimulation of the peroneal nerve by having the distal electrode too close to the peroneal region (Granat et al., 1993b). Attempts to limit this response by re-positioning the electrodes were not successful and, consequently, results for Subject 7 have not been included in these data sets.

The large variability between subjects limits the usefulness of the ensemble averaged curves illustrated in Figure 7.3.1.3. While it is clear from this figure that the model does not provide a satisfactory match to measured data, the reasons for this are masked amongst individual differences. Further discussion will therefore focus upon individual subjects.

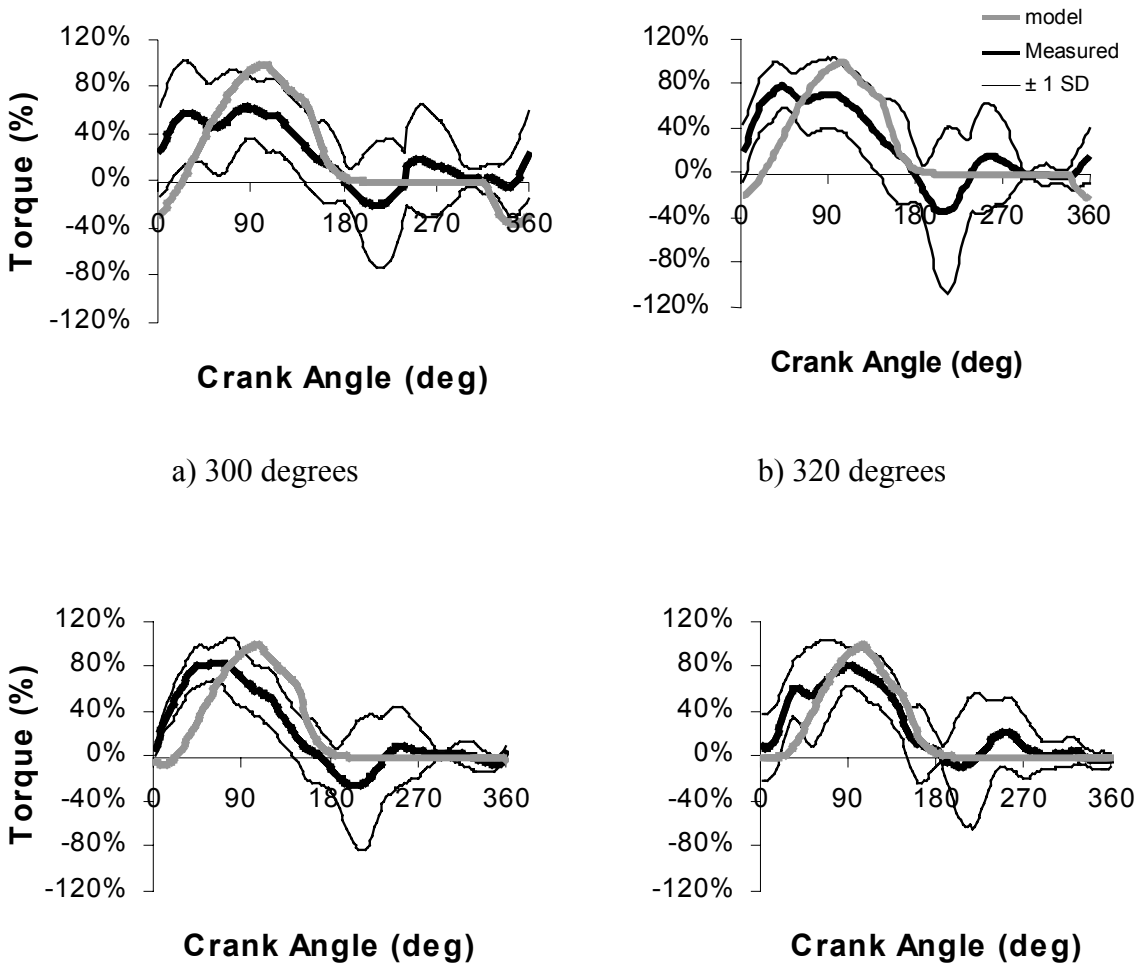

a) 300 degrees

b) 320 degrees

c) 340 degrees

d) 360 degrees

Figure 7.3.1.3 Average modelled and measured crank torque curves at selected angles of hamstring stimulation onset.

Pedal Forces

The model always predicted that subjects would push down and backwards on the pedal during the first quadrant after TDC (ie vertical and horizontal forces respectively positive and negative). Some subjects produced pedal force patterns quite similar to those predicted by the model, however the tendency for forces to oscillate after NMES cessation was present with the hamstring muscles as it was for the quadriceps (Figure 7.3.1.4). Other subjects demonstrated horizontal pedal forces in entirely the opposite direction to that predicted by the model (Figure 7.3.1.5)

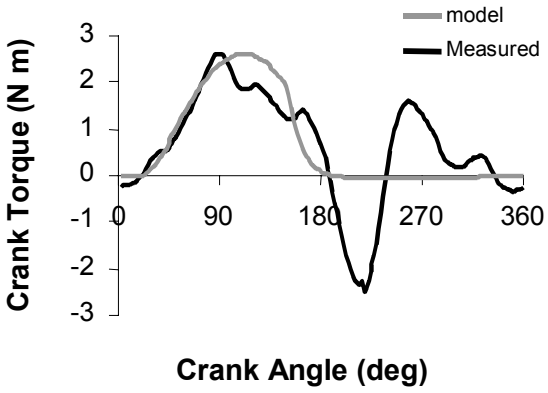

a) Torque

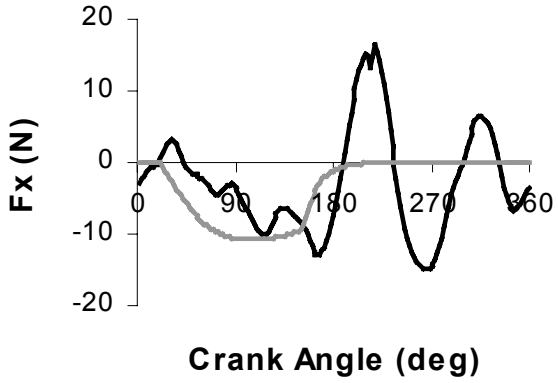

b) Horizontal Force

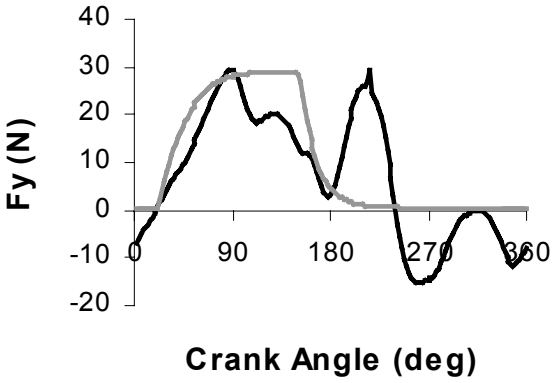

c) Vertical Force

Figure 7.3.1.4 Crank torque and pedal forces for Subject 3 with NMES firing angles between 0 and 120 deg.

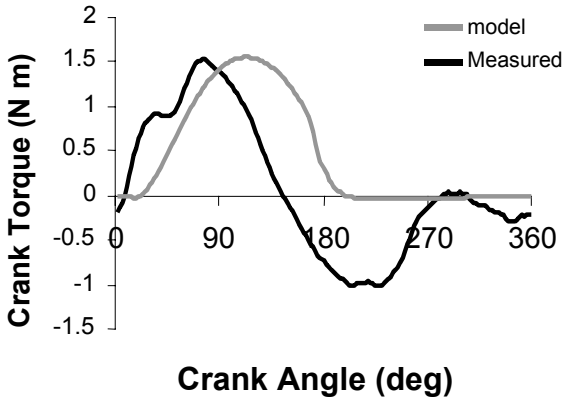

a) Torque

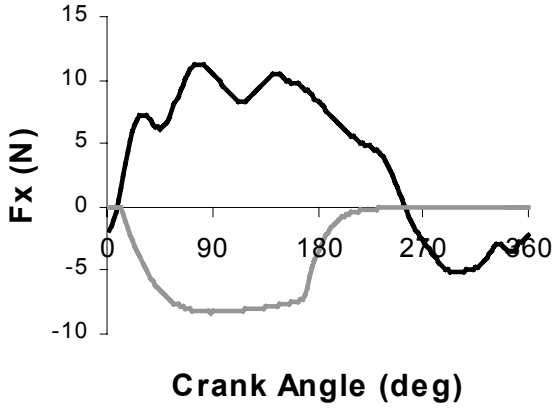

b) Horizontal Force

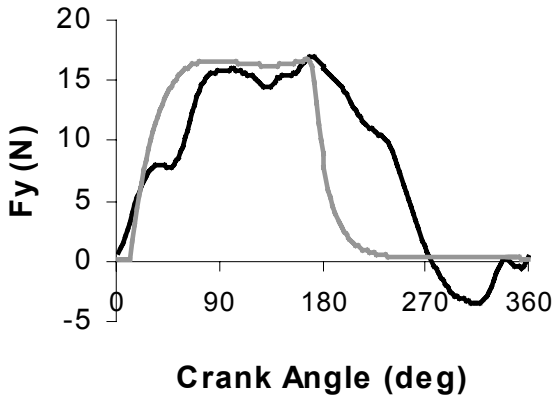

c) Vertical Force

Figure 7.3.1.5 Crank torque and pedal forces for Subject 4 with stimulation firing angles between 0 and 120 deg.

In order to produce the negative horizontal force predicted by the model, the hamstrings would have to flex the knee forcefully to pull back on the pedal. A measured positive pedal force, however, shows that the hamstrings were not flexing the knee to pull back as forcefully as they were causing the hip to extend and push the pedal forward. This result suggests that the model's moment arms about the hip and knee may have been inappropriately scaled, resulting in an incorrect balance between hip extension and knee flexion torques. Decreasing the model's knee moment arm by 40% produced a much better match to this subject's experimental data as demonstrated by Figure 7.3.1.6. This change in knee moment arms

improved the fit of the crank torque data as well, with correlations between measured and modelled torque increasing from 0.50 for Figure 7.3.1.5 to 0.86 for Figure 7.3.1.6.

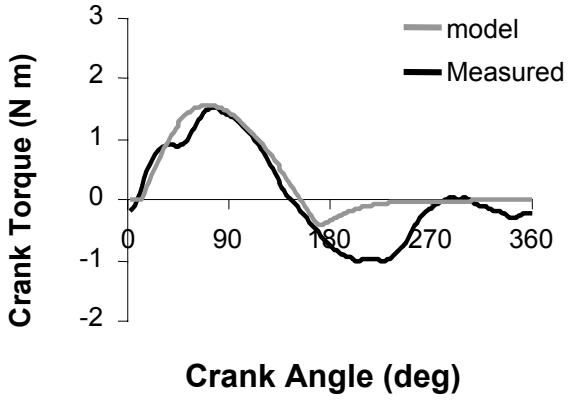

a) Torque

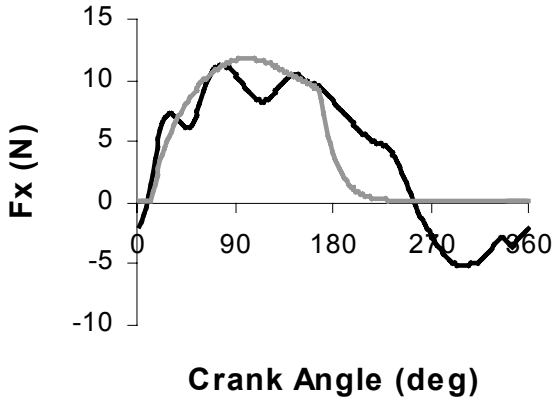

b) Horizontal Force

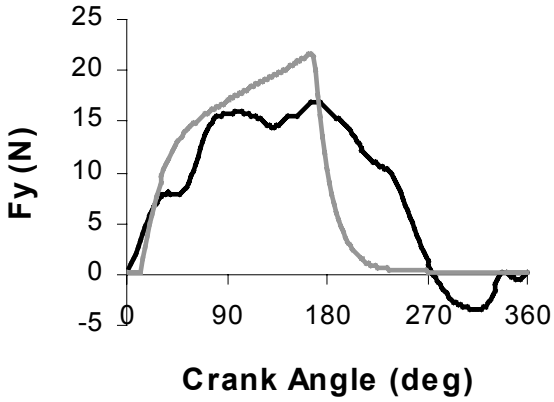

c) Vertical Force

Figure 7.3.1.6 Forces and torques for Subject 4 adjusted by decreasing the model's knee moment arm by 40% (For comparison with Figure 7.3.1.5)

Adjusting the model's hamstring moment arm about the hip can produce an almost identical pedal force output to changing the moment arm about the knee (Figure 7.3.1.7). Horizontal pedal force after TDC is determined by the relative effects of hip extension pushing forward and knee flexion pulling back on the pedal, hence it is the ratio between moment arms at the hip and knee that is important. Changing moment arms will, of course, affect other model

parameters such as the velocity of fibre shortening and subsequent muscle force. Figure 7.3.1.7, however, suggests that these have only a minor effect on the resulting pedal forces.

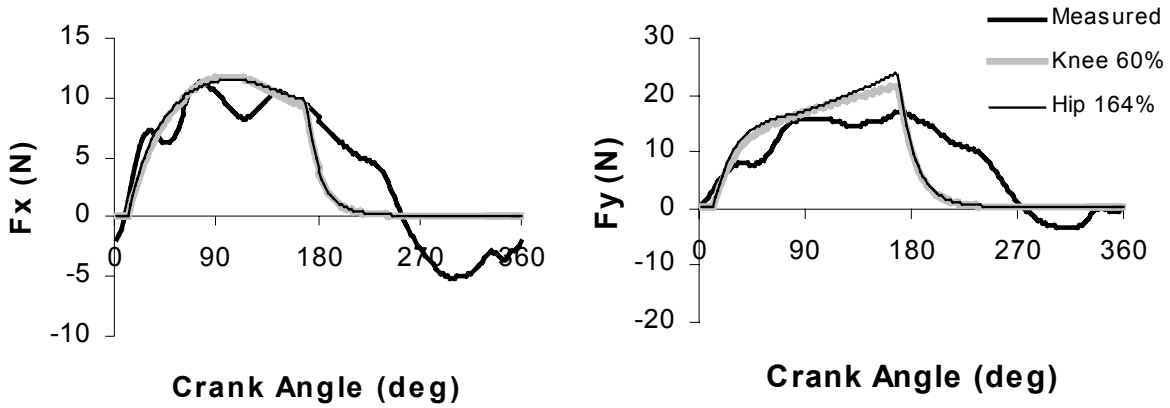

a) Horizontal Force b) Vertical Force

Figure 7.3.1.7 Comparison between pedal forces modelled using either a modification of knee or of hip moment arms.

Crank torques from Subject 1 consistently showed a large "dip" in torque around 70 deg for all trials examined. Figure 7.3.1.8 demonstrates that this reduction in crank torque was not the result of pedal forces being reduced by the motor suddenly dropping resistance. Rather, force was being applied to the pedal, but not in an appropriate direction to consistently generate propulsive torque.

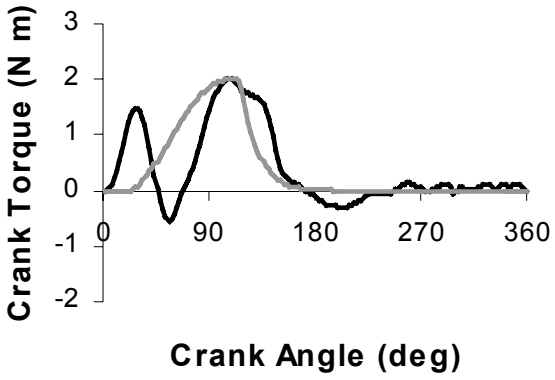

a) Torque

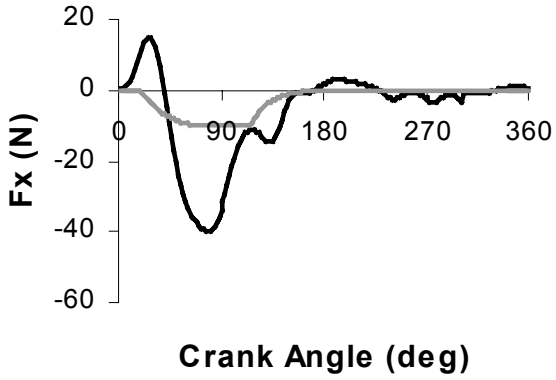

b) Horizontal Force

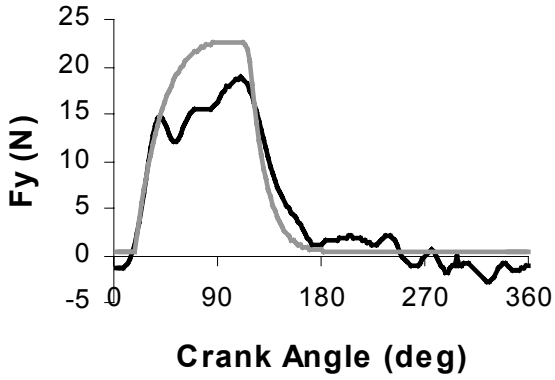

c) Vertical Force

Figure 7.3.1.8 Crank torque and pedal forces for Subject 1 with NMES firing angles of 0 to 90 deg.

Once again, manipulating the model's moment arm for the hamstring muscles at the knee can reduce the discrepancy between measured and modelled data. When knee moment arm was increased by 25%, this increased the negative horizontal force produced around 90 deg and generated negative torque followed by a subsequent positive torque (Figure 7.3.1.9). For this subject, increasing the hamstrings' moment arm about the knee increased the correlation between measured and modelled crank torques from 0.40 to 0.49.

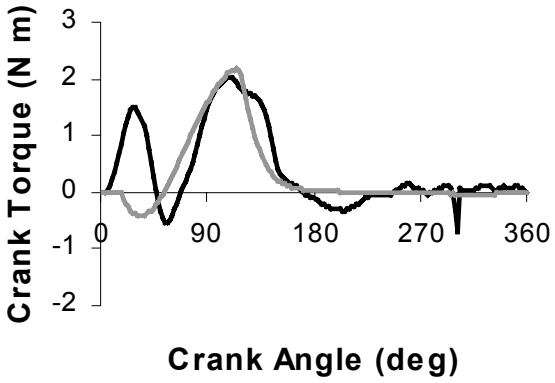

a) Torque

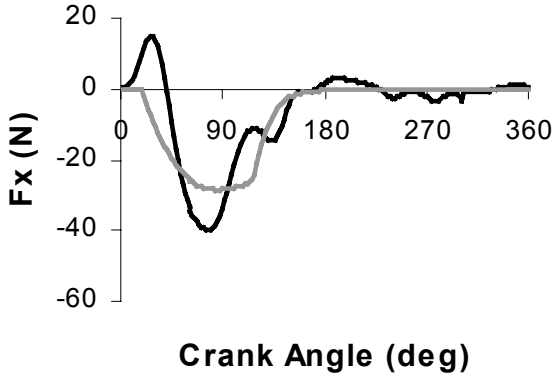

b) Horizontal Force

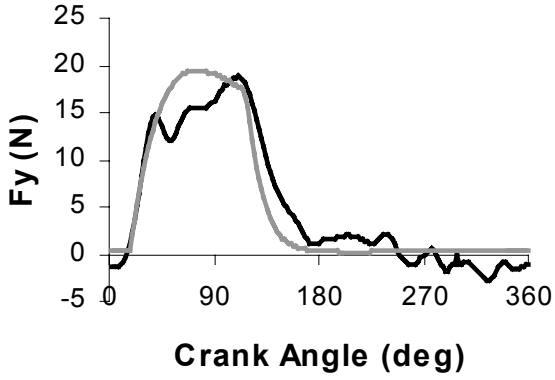

c) Vertical Force

Figure 7.3.1.9 Forces and torques for Subject 1, adjusted by increasing the model's knee moment arm by 25%

There was very little rebound following torque decline for Subject 1, hence the correlation between measured and modelled torque was primarily affected by the values within the active phase of each revolution. Note that, in Figure 7.3.1.9b, the measured horizontal pedal force was initially positive before changing to negative. This result could arise if the pattern of moment arm change with knee angle was not proportional to that which was modelled. Moment arms in Figure 7.3.1.9 were adjusted by making a proportional increase at every knee angle. If knee moment arms were initially reduced for positions before a crank angle of 30 deg (knee angle > 75 deg) and later increased at more extended knee angles, then the

measured data could have been matched even more precisely. This highlights the need for accurate, subject specific moment arm data.

Knee moment arms for every subject were systematically changed by increasing or decreasing the moment arm, proportionally at all knee angles, to match modelled pedal forces with measured values from a single trial for each subject (stimulation commencing at 0 deg). This procedure modified knee moment arms, to the nearest 5% of the original value, to minimise the sum of squares difference between measured and modelled pedal forces in the vertical and horizontal directions. Table 7.3.1.1 demonstrates that modifying the model's moment arm for the hamstring muscles across the knee increased the correlation between measured and modelled crank torques for every subject except Subject 3. The original moment arm equation produced the best fit between measured and modelled pedal forces for Subject 3, hence there was no modification performed for that subject.

Table 7.3.1.1 Correlations between measured and modelled crank torques when hamstring stimulation commenced at 0 deg.

Subject	Moment arm adjustment*	Correlation using standard moment arms	Correlation using adjusted moment arms
1	125%	0.40	0.49
2	60%	0.53	0.75
3	100%	0.50	0.50
4	60%	0.42	0.86
5	70%	0.17	0.51
6	85%	0.83	0.93
Average	85%	0.47	0.67

* Knee moment arms are given as a percentage of the original moment arms adapted from Buford et al. (1997).

7.3.2 Effect of changing stimulation onset angle

Measured Power Output

Figure 7.3.2.1 illustrates the average power output measures taken from four subjects plotted against hamstring stimulation commencement angle. Not all subjects have been shown on this figure for clarity of presentation, however data from all subjects may be found in Appendix 4.2.2. The arrows on Figure 7.3.2.1 illustrate the order of trials for each firing angle. As with the quadriceps muscle, stimulating the hamstring muscles produced a quadratic trend for firing angle superimposed over a definite order effect. Again, these two effects were partitioned out using multiple regression for both firing angle and trial number using Equation 7.2.3.1. Results for the regression analysis are shown in Table 7.3.2.1.

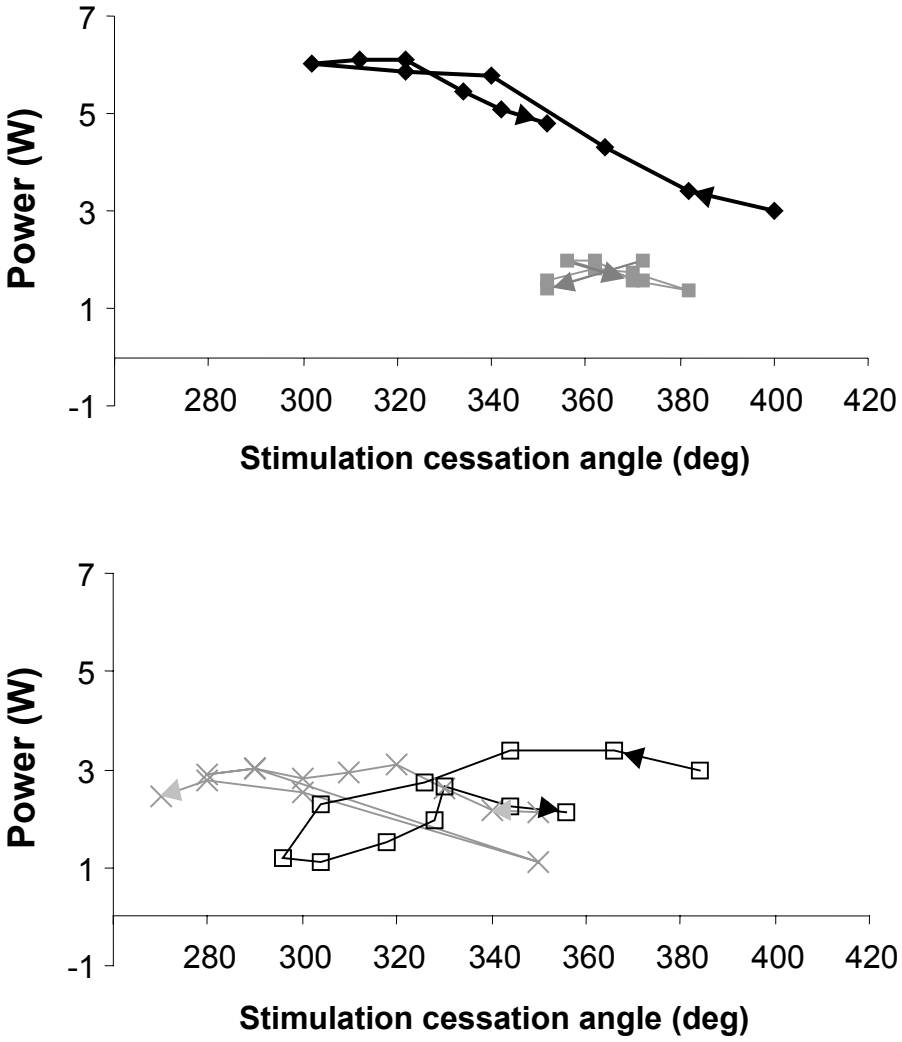

Figure 7.3.2.1 Change in power output with hamstring NMES onset angle for four representative subjects. See text for details

Table 7.3.2.1 Constants for Equation 7.2.3.1 from Analysis of Regression predicting power output from hamstring stimulation onset angle.

			Asymptotic 95 % Confidence Interval	
Constant	Estimate	Asymptotic Std. Error	Lower	Upper
A	0.035	0.056	-0.077	0.147
B	-0.00007	0.00008	-0.00023	0.00010
c_1	-3.3	9.5	-22.4	15.8
c_2	-2.8	9.6	-22.1	16.5
c_3	-2.1	9.5	-21.1	16.9
c_4	-4.5	9.5	-23.6	14.6
c_5	-0.1	9.5	-19.1	19.0
c_6	-1.3	9.4	-20.2	17.5
d_1	0.000	0.061	-0.122	0.122
d_2	-0.008	0.058	-0.125	0.109
d_3	-0.234	0.561	-1.358	0.889
d_4	0.000	0.071	-0.141	0.141
d_5	0.000	0.054	-0.108	0.108
d_6	-0.025	0.061	-0.148	0.098

Unlike the quadriceps muscles, stimulating the hamstrings produced a variable response for each subject. Figure 7.3.2.1 shows individual subjects clearly peaking at different stimulation onset angles. Equation 7.2.3.1 was designed to find a single stimulation firing angle resulting in maximum power output for all subjects. Applying Equations 4.4.4.4 to 4.4.4.6 to values from Table 7.3.2.1 gives a peak stimulation onset angle of 262 deg. This is clearly not an acceptable solution, being outside the range of values tested for all subjects. Applying

Equations 4.4.4.4 to 4.4.4.6 to estimate the uncertainty in peak angle gives uncertainties of 320 and 420 deg for constants a and b respectively. In other words, the regression procedure indicates that, based on the data available, the peak angle might be any crank angle. Testing a much wider range of angles would have reduced this uncertainty somewhat by generating very small or negative power outputs at more extreme firing angles. It is clear however, from viewing Figure 7.3.2.1, that with some subjects peaking at angles less than 300 deg while others peak around TDC, the average power for all subjects remains relatively constant across this range.

Analyses of regression were performed using Equation 7.2.3.1 individually for each subject. Peak angles calculated from the regression analysis for each subject are shown in Table 7.3.2.2. For Subjects 4 and 5, there were not enough stimulation angles tested on either side of the peak angle, which meant that the regression analysis was unable to find a meaningful peak for these subjects. Angles were calculated by the regression analysis, however visual inspection of Figure 7.3.2.2 indicates that they were clearly unreasonable estimates. Peak angles for the other four subjects appear reasonable from Figure 7.3.2.2, however care must be exercised in accepting these because the uncertainty estimates are still very high.

Table 7.3.2.2 Hamstring onset angles resulting in maximum power output calculated from individual regressions for each subject.

Subject	Stimulation onset angle	Uncertainty due to constant a	Uncertainty due to constant b
1	365	169	168
2	294	90	85
3	361	233	283
4	27*	2763	217
5	261*	714	588
6	322	60	57

* Peak angles from regression analysis were outside the range of angles tested for these subjects.

Prediction of peak stimulation firing angle from computer simulations.

The model's optimising routine found the average angle of stimulation cessation to maximise power output was 341 deg, with all subjects being within 10 deg of this angle. The 341 deg prediction fits right in the midst of the experimental values illustrated in Figure 7.3.2.1. Furthermore, if regression results from Subjects 4 and 5 are ignored, the model's predicted angle is within 5 deg from the average angles produced by regression analyses from the other four subjects (Table 7.3.2.2).

While the model seems to predict the group average peak stimulation onset angle, individual variation between subjects was not well predicted by the standard model (Figure 7.3.2.2). It appears that modelling individual kinematic parameters, while keeping a constant muscle model does not account for a large percentage of individual variation. In Section 7.3.1 it was shown that modifying the model's knee moment arm equation could improve the model's ability to predict the crank torques resulting from stimulation of the hamstring muscles. Table 7.3.2.3 shows for each subject; the knee moment arm size, peak stimulation onset angles measured from the analyses of regression, peak stimulation onset angle predicted by the

standard model and the angle predicted by the model with modified knee moment arms. This information is further illustrated by Figure 7.3.2.2, together with the power outputs measured at each firing angle for all subjects.

Table 7.3.2.3 Peak hamstring NMES onset angles measured by analysis of regression and predicted by the standard and modified models.

Subject	Measured Peak Angle	Angle predicted by Standard Model	Angle predicted using Adjusted moment arms	Size of moment arm adjustment
1	365	343	373	125%
2	293	346	305	75%
3	361	331	331	100%
4*	260	341	293	60%
5*	26	349	307	70%
6	322	345	317	80%

* Regression analysis was unable to find a maximum value within the range of angles measured for these two subjects.

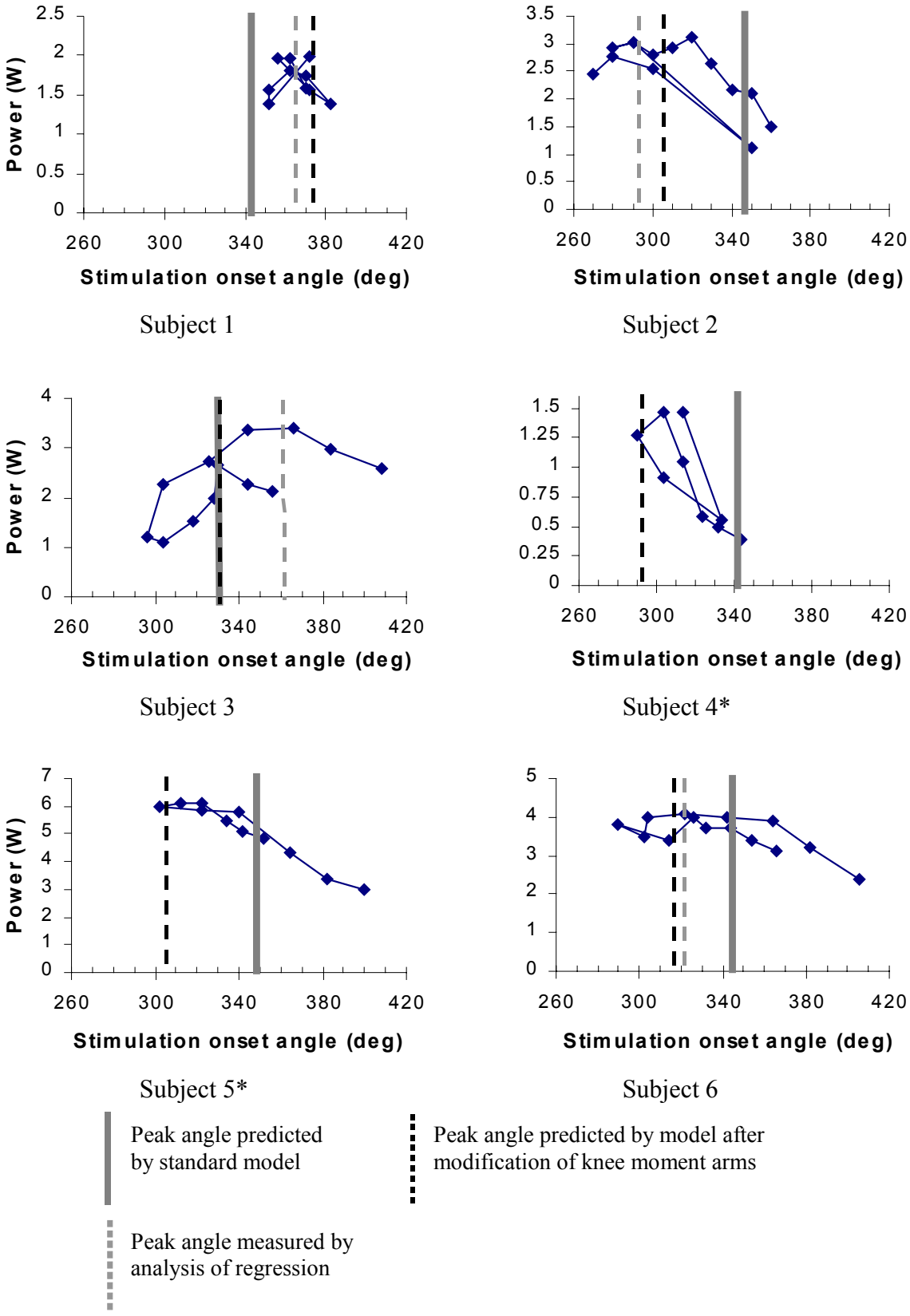

Figure 7.3.2.2 A comparison between measured and predicted NMES onset angles that maximise power output by the hamstring muscles.

* Regression analysis was unable to find a maximum value within the range of angles measured for subjects 4 and 5.

It can be seen from Table 7.3.2.3 and Figure 7.3.2.2 that, again except for Subject 3, individual modification of the model's moment arm for the hamstring muscles across the knee improved the model's performance. The optimum stimulation firing angle for individual subjects was poorly predicted by the standard model, however modification of individual knee moment arms remarkably improved the model's predictive ability.

7.3.3 Effect of changing stimulation cessation angle

Measured Power Output

Like stimulation onset angle, changing stimulation cessation angle produced relatively small changes in average power output (Figure 7.3.3.1). Analysis of regression (Table 7.3.3.1) found the common stimulation cessation angle producing peak average power output to be 155 deg. The uncertainty arising from constants a and b in Equation 7.2.3.2 was calculated to be 54 and 57 deg respectively.

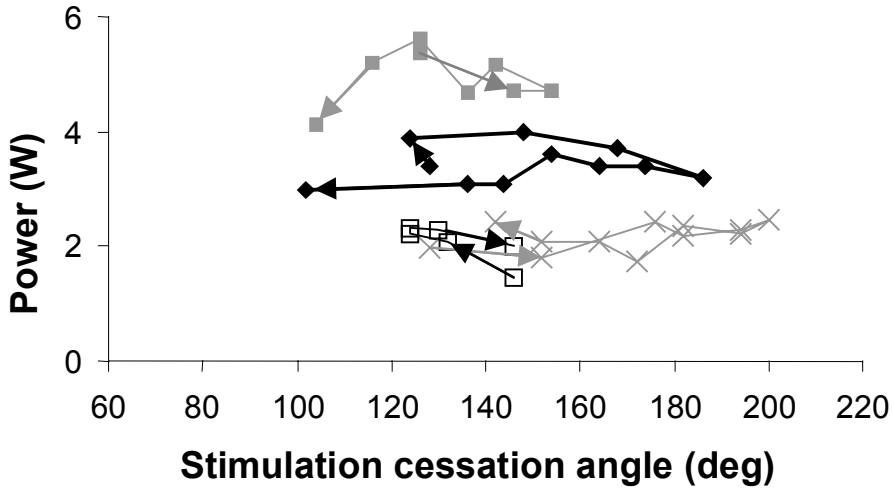

Figure 7.3.3.1 Change in power output with hamstring NMES cessation angle for four representative subjects. See text for details

Table 7.3.3.1 Constants for Equation 7.2.3.1 from Analysis of Regression predicting power output from hamstring stimulation cessation angle.

			Asymptotic 95 % Confidence Interval	
Constant	Estimate	Asymptotic Std. Error	Lower	Upper
a	-0.073	0.025	-0.124	-0.021
b	0.00023	0.00009	0.00006	0.00041
c_1	6.7	1.8	2.9	10.4
c_2	8.4	1.9	4.5	12.3
c_4	8.3	1.7	4.8	11.8
c_5	9.8	2.0	5.7	13.9
c_6	6.6	1.9	2.7	10.5
d_1	0.000	0.037	-0.074	0.074
d_2	-0.103	0.153	-0.415	0.209
d_4	-0.253	0.754	-1.787	1.280
d_5	-0.129	0.235	-0.606	0.348
d_6	0.000	0.104	-0.211	0.211

Individual regressions were performed for each subject. While the peak angles found by the regression equations coincide with a visual inspection of the data, the uncertainties inherent in the individual regression constants are again quite substantial (Table 7.3.3.2, Figure 7.3.3.2).

Table 7.3.3.2 Hamstring cessation angles resulting in maximum power output calculated from individual regressions for each subject.

Subject	Stimulation cessation angle	Uncertainty due to constant a	Uncertainty due to constant b
1	150	-198	-179
2*	12	1197	131
3			
4	118	461	401
5	130	57	56
6	149	113	116

* Peak angles from regression analysis were outside the range of angles tested for this subject.

** No stimulation cessation angles were measured for this subject.

Prediction of peak stimulation cessation angle from computer simulations.

The model was used to predict stimulation cessation angles generating peak average power output using both standard and modified moment arms for the hamstrings across the knee. Once again, the moment arm modifications substantially improved the ability of the model to match individual variations in peak cessation angles (Table 7.3.3.3). The modified moment arm model predicted a peak angle much closer to the peak identified by regression analysis for all subjects except Subject 1. While the original model predicted a peak angle closer to that measured by regression, visual inspection of Figure 7.3.3.2a suggests that the regression angle may not be the true peak angle for that subject. Such a result is possible given the multiple variables used in the regression combined with the relatively small number of data points. If the analysis calculates inappropriate fatigue constants, this will affect determination of the angle constants.

Table 7.3.3.3 Peak hamstring NMES cessation angles measured by analysis of regression and predicted by the standard and modified simulations.

Subject	Measured Peak Angle	Angle predicted by Standard Model	Angle predicted using Adjusted moment arms	Size of moment arm adjustment
1	150	166	187	125%
2*	12	166	132	75%
3**		156	156	100%
4	118	165	122	60%
5	130	172	130	70%
6	146	168	152	80%

* Regression analysis was unable to find a maximum value within the range of angles measured for this subject.

** No stimulation cessation angles were measured for this subject.

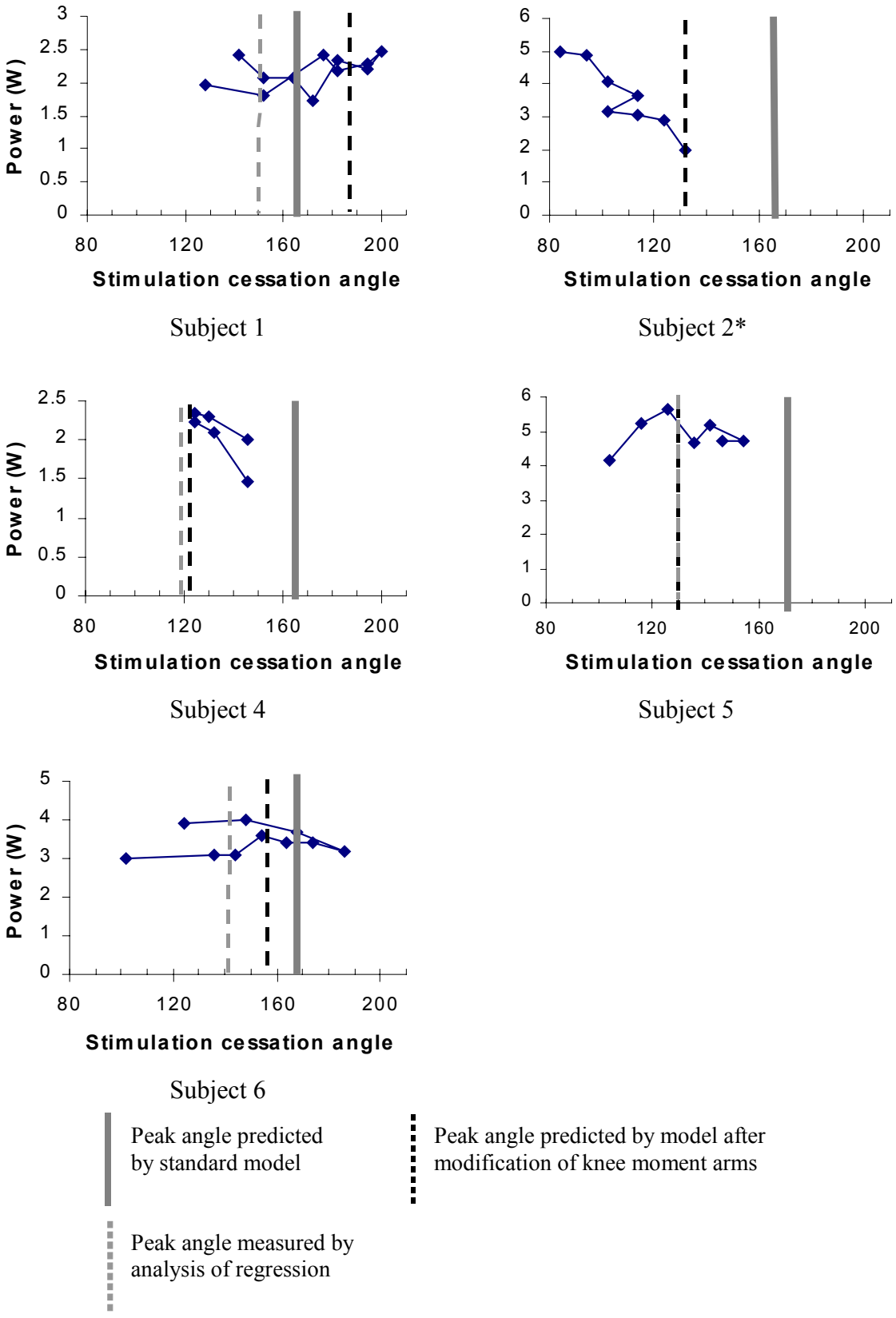

Figure 7.3.3.2 A comparison between measured and predicted NMES cessation angles that maximise power output by the hamstring muscles.

* Regression analysis was unable to find a maximum value within the range of angles measured for subject 2.

7.3.4 Discussion

All muscles in the hamstring group except the short head of biceps femoris cross both the hip and knee. The performance of the hamstring group is therefore determined by movements at both the hip and knee joints, proportionally, according to relative moment arms about the hip and knee. Any change in the relative hip and knee moment arms between individuals will cause a corresponding change in muscle performance. This is evidenced in the present study whereby different subjects require different stimulation firing angles to produce their maximum power output. Inter-subject differences cannot be explained just by considering limb lengths and seating positions. Models must use moment arms that are tailored to specific subjects if individual variations are to be considered.

The above finding is in contrast to the quadriceps muscles, which demonstrated relatively similar firing angles for all subjects. For the quadriceps, only rectus femoris crosses the hip and this muscle has the smallest cross sectional area. Optimum firing angles are therefore determined primarily by movements at the knee with little contribution from the hip. Consequently, inter-subject differences in hip-knee moment arm ratios cause little difference in optimum firing angles for the quadriceps; rather the firing angles are determined simply by the angle at which the knee begins to extend. While individual anthropometrics change the range of knee flexion experienced by each subject, and moment arm differences affect the amount of torque produced by each subject; the knee begins to extend at a similar crank angle for all subjects and consequently the quadriceps firing angles are similar.

There have been wide ranges of moment arms reported for different muscles in the hamstring group (Figure 7.3.4.1). The standard moment arm equation used for the present study was based on results from Buford et al. (1997). The single hamstring group moment arm was calculated from a weighted average of the four muscles taking into account their relative cross sectional areas and hence contribution to the overall muscle strength. In order to better match measured pedal forces, the standard moment arm calculated from Buford et al. was either increased or decreased by up to 40% (Table 7.3.2.3).

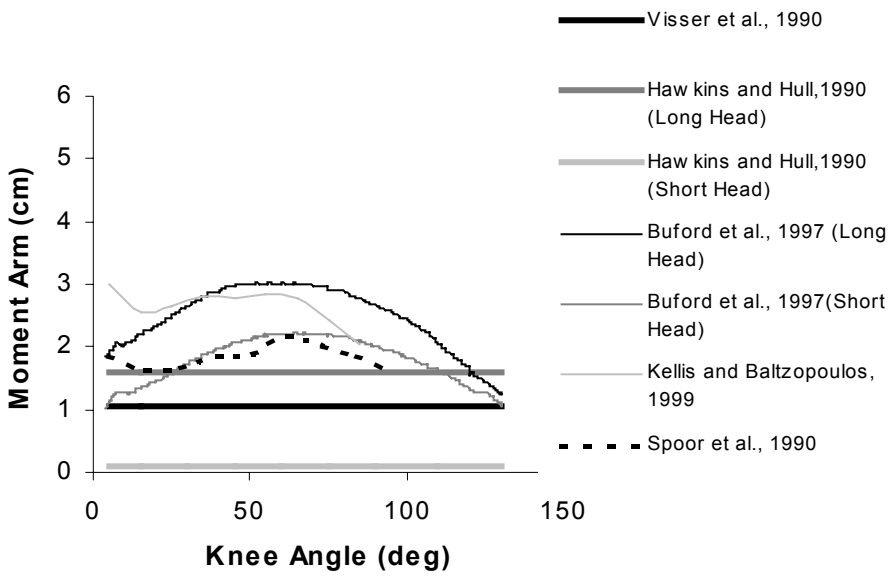

a) biceps femoris

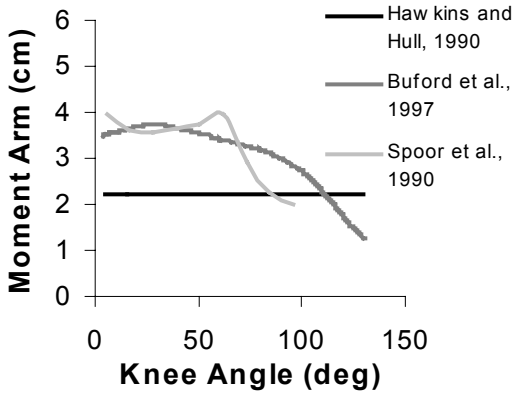

b) semimembranosus

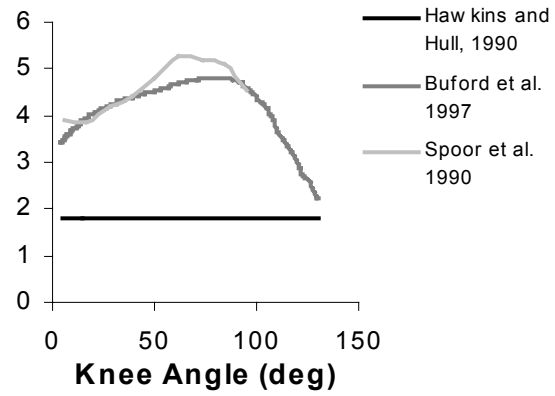

c) semitendinosus

Figure 7.3.4.1 Range of moment arm values available for each hamstring muscle from different literature sources.

Knee moment arms within the present model were adjusted to provide a closer match between measured and modelled pedal forces. It is possible that the inter-subject differences may represent only apparent moment arms for the hamstring group, rather than actual differences in moment arms between subjects. This situation may arise because it is likely that not all muscles within the hamstring group were being stimulated with equal intensity. Furthermore, subjects may have different relative cross sectional areas between muscles to those used in the partitioning of relative force. Any differences in the relative strength of contractions produced

by a subject's muscles may be seen as a difference in moment arm for the whole group, because the group moment arm is not representative of any particular muscle. For example, semitendinosus generally has a larger moment arm than the other hamstring muscles. If one subject had either preferential stimulation of this muscle resulting from electrode placement, or a stronger semitendinosus than did all other subjects, then this would mean that a greater percentage of the hamstring force for this subject would be transmitted across a larger moment arm. Forces for this subject would therefore be more accurately predicted using a larger moment arm for the whole hamstring group.

Only proportional changes across all knee angles were made to the moment arm functions derived from Buford et al. (1997). That is, the entire curve illustrated in Figure 7.3.4.1 was moved up or down by a certain percentage without changing the relative differences between joint angles. In practice, each subject is likely to differ slightly in the change between joint angles as well as in average magnitude. Further refinements in individual moment arm calculations would therefore be likely to improve the model's ability to make predictions for individual subjects.

Moment arms for hamstring muscles across the hip have been left constant, with only knee moment arms to match experimental data. Making proportional changes to the hip moment arms instead of the knee had a very similar effect on the resulting pedal forces, with horizontal pedal force after TDC being determined by the relative effects of hip extension pushing forward and knee flexion pulling back on the pedal. While it has been shown that changing hip moment arms can produce almost identical pedal force graphs to changing knee moment arms, the effect on the muscle was not considered. The hip and knee both extend across the top of each pedal revolution while the hamstring muscle is stimulated. These joint movements have opposite effects on hamstring muscle length, however. Because the hamstrings have larger moment arms across the hip, the muscle shortens during this phase and thus is able to generate positive work. Reducing the moment arm about the knee would reduce the lengthening effect of knee extension and thus result in a higher velocity of contraction. Increasing the moment arm about the hip would have the same effect on contraction velocity, and this would have two effects on muscle performance. Firstly, increased contraction velocity would make it more difficult for muscles to generate a given level of force, requiring a greater level of stimulation. Secondly, for the same level of force, higher velocity would result in a higher power output of the muscle with correspondingly increased energy cost. Of

course, inter-subject variability in moment arms is likely to be accompanied by variability in fibre length as well, which may negate the moment arm differences. This highlights the desirability, discussed in Section 6.1.7, of having all model parameters matched to one another.

The NMES firing angles that resulted in maximum power output by the hamstring muscles varied between individuals. This variability in individual responses prevented the analysis of regression method from determining a reasonable peak stimulation angle. Peak NMES onset angles for individuals varied between 293 and 373 deg when the model was adapted by modifying knee moment arms for individuals. Measured onset angles for individuals were subject to very high uncertainties, but showed agreement to the model by varying between 293 and 365 deg for the four subjects where analysis of regression was able to identify a peak angle within the range investigated (Table 7.3.2.3).

Modelled peak NMES cessation angles for individual subjects varied between 122 and 187 deg after modification of each individual's knee moment arm function. Again, this showed agreement to the measured variation between 118 and 150 deg for the four subjects available (Table 7.3.3.3). While there was considerable variation in peak NMES onset angles between individuals, a duty cycle of approximately 180 deg produced the maximum power output for each individual.

7.4 NMES firing angles to maximise power output by the gluteal muscles

7.4.1 Comparison of modelled to measured results.

Overview of crank torques produced by stimulation of the gluteal muscles.

The response of individual subjects to stimulation of the gluteal muscles was quite variable. As can be seen from Figure 7.4.1.1, some subjects produced relatively large torques in response to gluteal stimulation while others produced a negligible response, even when stimulation levels were turned up to the maximum current of 140 mA.

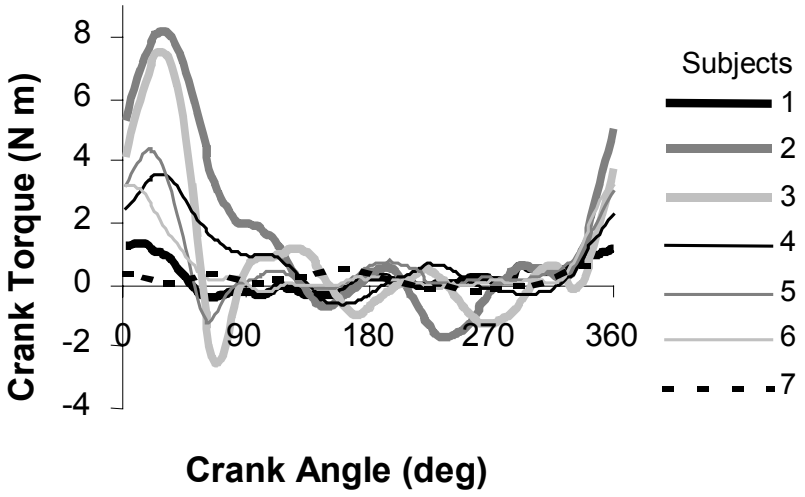

Figure 7.4.1.1 Non-normalised crank torques for individual subjects in response to stimulation of the gluteal muscles. Stimulation onset angle was 300 deg for all subjects, however stimulation ceased at varying angles for each subject between 20 and 80 deg.

All torques for hamstring and quadriceps muscles were normalised as a percentage of peak torque before investigating patterns in response to stimulation changes. For subjects producing only very small torques in response to gluteal stimulation, the normalising process greatly exaggerated the inevitable errors during the passive phase, masking any visible response to the stimulation. For this reason, two subjects (1 and 7) have been eliminated from further analyses of the response to gluteal stimulation.

Normalised crank torque for the other five subjects is illustrated in Figure 7.3.1.1. Note that there is considerable variability between individuals. Torque peaked at different crank angles for each subject. The simulations did not predict such marked individual variability (Figure 7.2.1.2).

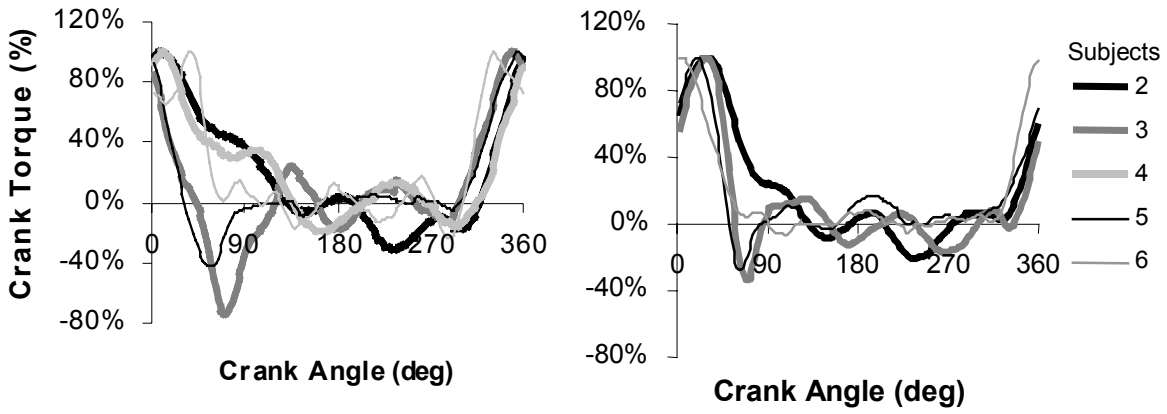

a) 260 deg b) 300 deg

Figure 7.4.1.2 Individual crank torque curves measured at selected gluteal NMES onset angles.

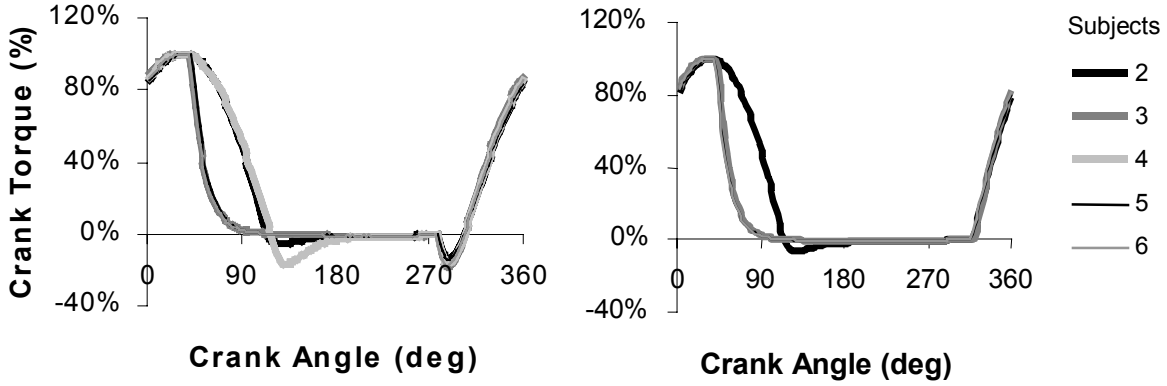

a) 260 deg b) 300 deg

Figure 7.4.1.3 Modelled crank torques for the same trials shown in Figure 7.3.1.1.

Crank torque peaked at different angles for each stimulation onset angle (Table 7.4.1.1). This is in contrast to results from the quadriceps muscles, where the angle of peak torque remained constant as stimulation onset angle changed. As stimulation commenced later, so too did the crank torque peak later. This suggests either that the gluteal muscles took a very long time to develop force, that the muscles were fatiguing when stimulated for too long, or both.

Table 7.4.1.1 Angle where torque was maximum for each subject at different stimulation onset angles.

	Stimulation onset angle			
Subject	240	260	280	300
2		368	378	390
3		348	370	388
4		370	388	360
5	340	356	368	380
6	388	330	344	364
Average		354.4	369.6	376.4

Note: Angles after TDC have had 360 deg added for ease of comparison with those angles found to be just less than TDC.

An example subject will be used to explain the above two possibilities. Subject 5, when stimulation commenced at 260 deg, reached peak torque at a crank angle of 356 deg. Let us consider, hypothetically, that it took a time equivalent to 100 deg of crank rotation (0.33 s) for the gluteal muscles to reach full activation; and that the crank angle giving the optimum combination of fibre length, fibre velocity, muscle moment arm, and effectiveness with which hip extension torque could generate crank torque was 360 deg. Under these conditions, stimulation commencing at 260 deg would just have time to reach full activation by the angle of maximum effectiveness. If stimulation commenced at 280 deg, by contrast, there would not be sufficient time for the muscle to reach full activation by the time the optimum angle was reached. Therefore, a different optimum angle would be expected that maximised activation as well as the other mentioned variables.

The alternative hypothesis was that muscles were fatiguing after a given period of continuous activation. To explain this, let us consider a hypothetical situation where full activation was

reached after a time equivalent to 60 deg crank rotation (0.2 s), however the muscle force began to decline through fatigue after 100 deg of rotation (0.33 s). Let us consider also that the optimum angle for fibre length, muscle moment arm, and hip torque effectiveness was 20 deg after TDC (380 deg on Table 7.4.1.1). In this case, although the most effective angle might be 20 deg, when stimulation commenced early at 260 deg, the muscle would have been active too long and hence force would be declining by the time the optimum angle was reached. Consequently, an earlier angle would be found for this stimulation onset angle. When stimulation commenced later at 300 deg, the 20 deg position would then be expected to generate peak torque because activation would be maximal at this angle without the contraction duration being so long as to induce significant fatigue.

Either or both of these options were possible, in fact different mechanisms may be dominant in different subjects. Neither hypothesis is supported by data from the knee extension experiments, because time to full activation was approximately 0.2 s (about 60 deg rotation) and muscle force did not decline through fatigue after 2 s of continuous isometric contraction. No data are available, however, for contractions of the gluteal muscles, hence these options cannot be ruled out.

Figure 7.4.1.4 illustrates the ensemble averaged measured torques compared to those predicted by the model. The model predicts the timing and direction of the initial movement away from zero for each of the stimulation firing angles illustrated by Figure 7.4.1.4. Firing angles generating initially negative torques are well matched between measured and modelled data. The crank angle where torque changed from negative to positive was matched to the nearest 4 deg and 2 deg respectively for the 240 and 260 deg firing angles. This match suggests that the model is able to predict when the gluteus maximus muscle fibres begin to shorten, and hence are able to generate positive power. This should then have enabled it to predict the peak stimulation onset angle.

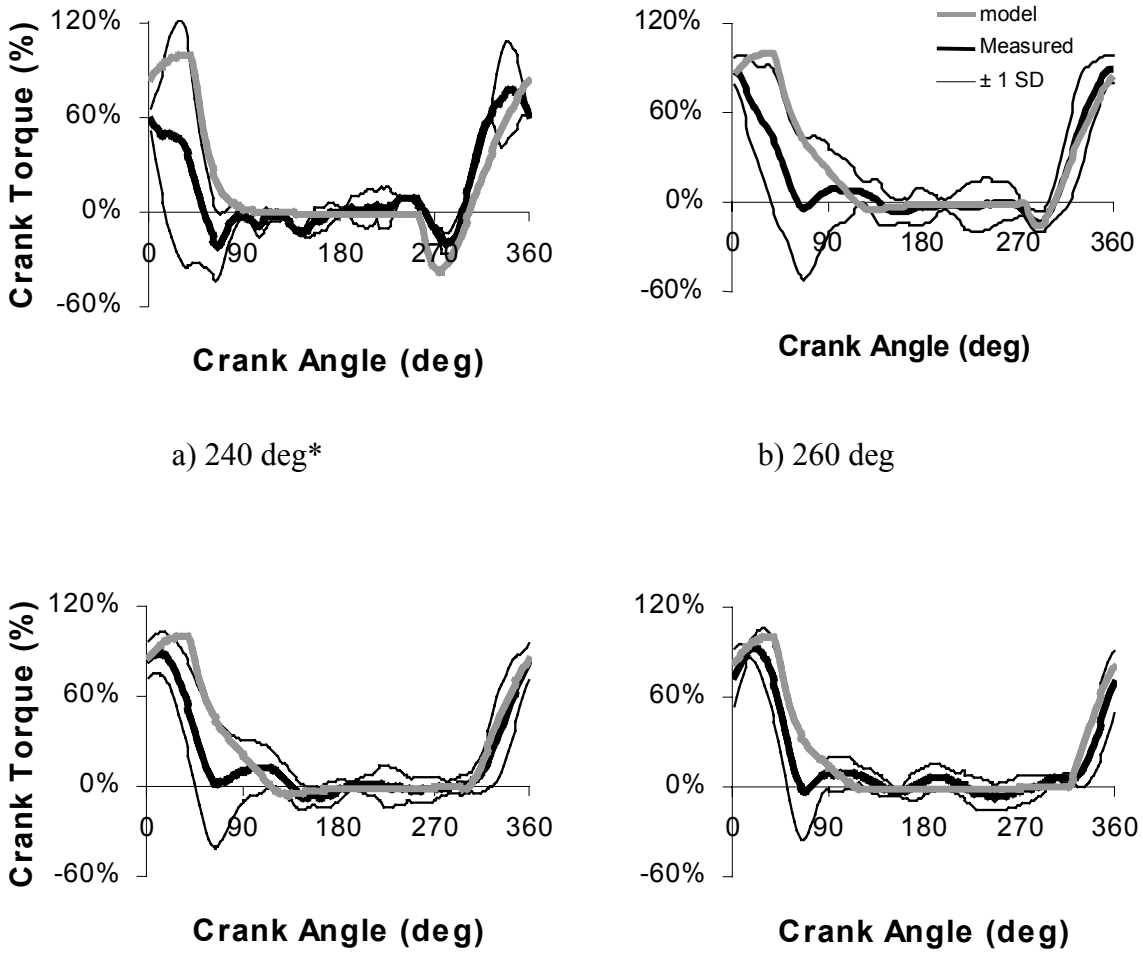

a) 240 deg*

b) 260 deg

c) 280 deg

d) 300 deg

Figure 7.4.1.4 Crank torques produced in response to stimulation of the gluteal muscles at different onset angles.

* This angle has been included to illustrate the negative torque period arising from early stimulation, however only two subjects were tested at this angle.

After the initial onset, modelled torques deviated substantially from the measured values (Figure 7.4.1.4). Rates of rise differed and peak torque occurred at a different angle in measured and modelled data. Modelled crank torque peaked at 34 deg after TDC for every stimulation firing angle, while Table 7.4.1.1 demonstrates that measured torque peaked earlier than this for every trial used to compile Figure 7.4.1.4.

A further explanation for differences between modelled and measured torque (but not for the changing angle of peak for individual subjects) is the lack of fit between modelled isometric hip extension torques, and those measured in-vivo via maximum voluntary contractions. As discussed in Section 6.2.2, a single representative fibre is unable to generate significant torque over a wide range of hip angles. Figure 7.4.1.5 shows that, around TDC, the hip was extending from a maximally flexed angle of 130 deg to an angle of 100 deg at the most extended position. The model suggests that gluteal force should have been increasing through this period because, although fibre length was shortening below optimal length, the muscle's moment arm was increasing at a greater rate to compensate. The model's peak hip extension moment for the gluteal muscles occurred at a hip flexion angle of approximately 53 deg. In-vivo measurements of hip extensor torque were not available from published literature for hip angles beyond 90 deg, however the measurements suggested a peak angle at or greater than 90 deg (Waters et al., 1974; Nemeth et al., 1983). The difference between measured and modelled crank angles producing maximum torque is therefore likely to result from this inability of the model to match in-vivo torque-angle measures. The present model's slack length could have been manipulated to produce maximal hip extensor torque at a greater angle of flexion. This would have meant, however, that the model would predict that no hip extensor torque could be generated at full extension. The present slack length appeared to be the best compromise within the constraints of the current single fibred model. To improve the ability of a model to predict hip extensor torques it would be necessary to model gluteus maximus as a multiple number of fibres. Multiple gluteal fibres, with individual lengths and moment arms for each fibre, would be able to generate torque over a wider range of hip angles than the present model. The distributed fibre model presented in Chapter 3 would not satisfy this need because all fibres in Chapter 3 were modelled to change length by an amount equal to the length change of the whole muscle.

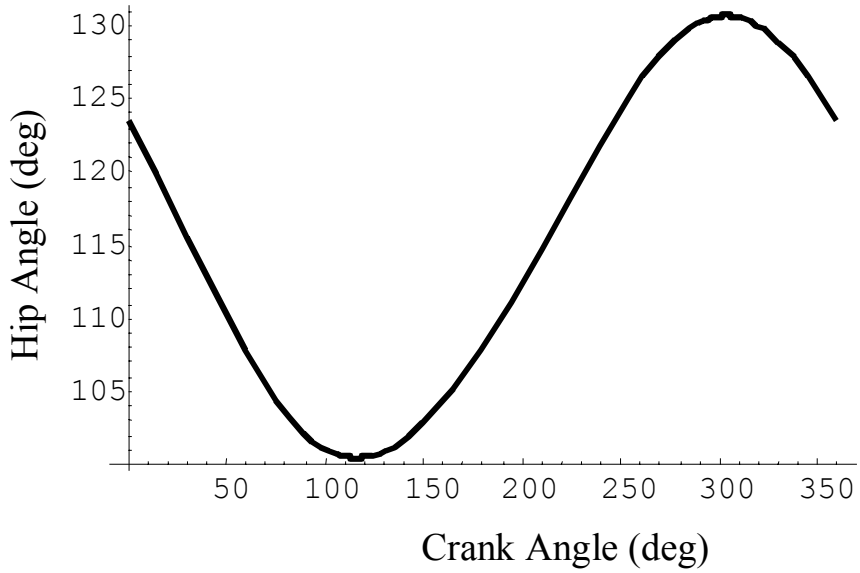

Figure 7.4.1.5 Hip angle for one representative subject plotted as a function of crank angle.

7.4.2 Effect of changing stimulation onset angle

Measured Power Output

Angle seeking experiments were performed for the gluteus maximus in a similar fashion to the other muscles. Figure 7.3.2.1 illustrates the changes in average power output with stimulation onset angle for four representative subjects. Again, not all subjects have been shown for clarity of the figures, however the full data set is available from Appendix 4.2.2. Similarly to the other muscles, the angle generating maximum power was identified through analysis of regression to identify constants for use in Equation 7.2.3.1 (Table 7.4.2.1). The peak angle identified was 305.8 deg, with an uncertainty of 80.8 and 86.3 deg for constants a and b respectively.

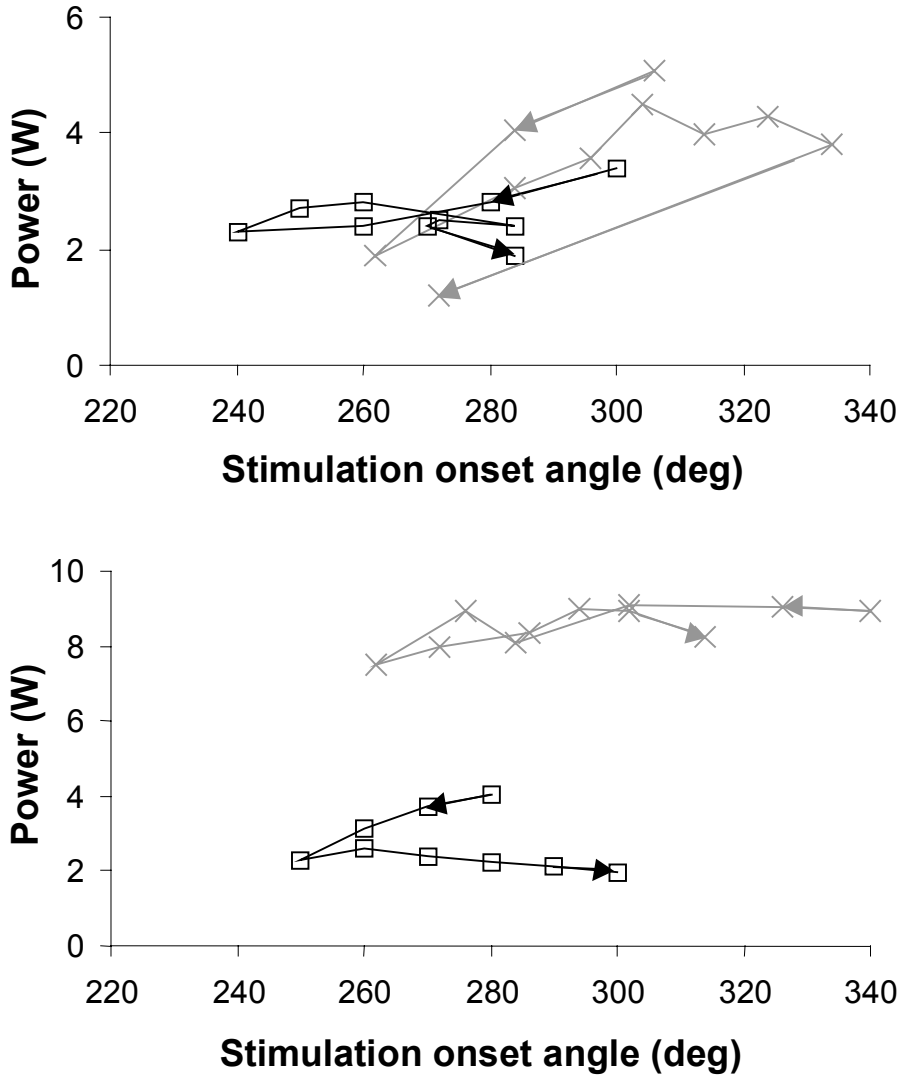

Figure 7.4.2.1 Change in power output with gluteal NMES onset angle for four representative subjects

Table 7.4.2.1 Constants for Equation 7.2.3.1 from Analysis of Regression predicting power output from gluteal stimulation onset angle.

			Asymptotic 95 % Confidence Interval	
Constant	Estimate	Asymptotic Std. Error	Lower	Upper
a	0.270	0.071	0.126	0.413
b	-0.00044	0.00012	-0.00069	-0.00019
c_2	-32.6	10.3	-53.3	-12.0
c_3	-37.5	10.1	-57.9	-17.2
c_4	-38.3	10.5	-59.4	-17.2
c_5	-38.5	10.7	-60.0	-16.9
c_6	-38.6	10.2	-59.1	-18.0
d_2	-0.246	0.616	-1.488	0.996
d_3	-0.228	0.701	-1.642	1.187
d_4	-0.225	0.943	-2.127	1.676
d_5	-0.142	0.558	-1.268	0.984
d_6	-0.103	0.252	-0.611	0.405

Prediction of peak stimulation firing angle from computer simulations.

As with the other muscles, simulations were performed at different stimulation firing angles to determine the onset angle that maximised power output to the crank. The peak firing angle was predicted to be 273 deg, with no subjects varying by more than 1 deg from this angle. While there appears to be a 30 deg difference in measured and modelled results, this is likely due to the precision of the measured regression equations rather than the model's inaccuracy. Figure 7.4.1.4 demonstrates that the model satisfactorily predicts both the cross-over from negative to positive torque at a crank angle of about 300 deg and the delay between

stimulation onset and torque rise. This enhances confidence in the model's ability to predict suitable firing angles because the peak onset angle is determined primarily by those two factors.

7.4.3 Effect of changing stimulation cessation angle

Measured Power Output

Power outputs resulting from changes in gluteal stimulation cessation angle are illustrated for four subjects in Figure 7.3.3.1. Analysis of regression failed to bracket a suitable maximum stimulation cessation angle. Applying Equations 4.4.4.4 to 4.4.4.6 to constants from Table 7.4.3.1 gave a peak cessation angle of –147 deg with uncertainties of 266 and 463 deg from constants a and b. This result is clearly not meaningful, indicating that there was no consistent angle giving peak power output across the range of cessation angles examined.

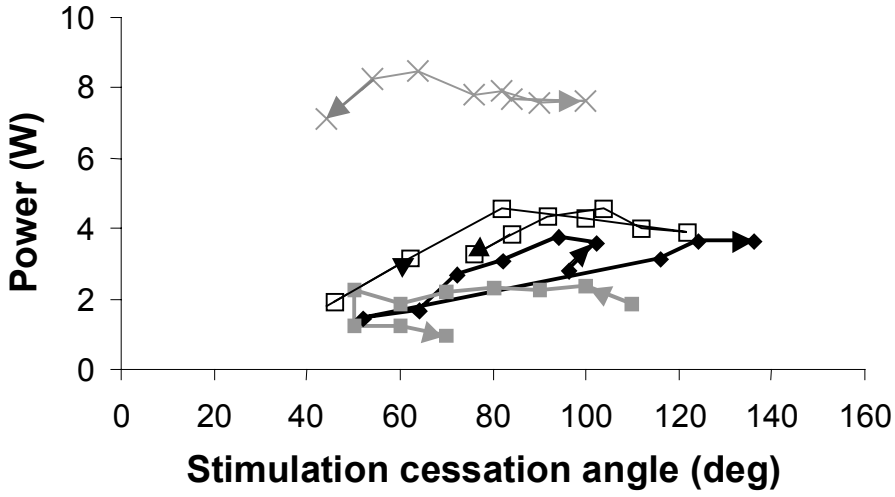

Figure 7.4.3.1 Change in power output with gluteal NMES cessation angle for four representative subjects

Table 7.4.3.1 Constants for Equation 7.2.3.1 from Analysis of Regression predicting power output from gluteal stimulation cessation angle.

			Asymptotic 95 % Confidence Interval	
Constant	Estimate	Asymptotic Std. Error	Lower	Upper
a	0.011	0.020	-0.029	0.051
b	0.00004	0.00012	-0.00020	0.00027
c_2	5.30	0.99	3.29	7.31
c_3	1.24	0.83	-0.46	2.93
c_4	0.00	0.97	-1.98	1.97
c_5	1.09	1.17	-1.29	3.46
c_6	1.09	1.21	-1.39	3.56
d_2	0.082	0.044	-0.007	0.172
d_3	0.039	0.037	-0.037	0.114
d_4	-0.033	0.084	-0.204	0.139
d_5	-0.130	0.279	-0.697	0.438
d_6	-0.345	1.333	-3.056	2.366

Prediction of peak stimulation firing angle from computer simulations.

Computer simulations predicted 85 deg as the cessation angle giving maximum power output. Inter-subject variability in simulations was small with all simulations within 5 deg from this average. This cessation angle cannot be verified from the regression analysis, however 85 deg is close to 180 deg out of phase from the modelled peak onset angle.

7.4.4 Summary

Individual responses to gluteal muscle stimulation were quite variable with some subjects applying no measurable torque to the crank under maximum stimulation while others produced substantial torque with smaller stimulation levels. It is possible that this variability resulted from placement of electrodes over the muscle, however those subjects producing little or no torque did so consistently at two successive testing sessions. It therefore seems more likely that the lack of response from some subjects was the result of a high threshold of activation (Lieber and Kelly, 1991). While this precise physiological cause of this variability is unknown, Lieber and Kelly suggest that it may be related to the proximity of motor nerves to the skin for each individual.

Computer simulations provided a satisfactory match between measured and modelled crank torques during the initial rise of torque following stimulation onset. The model predicted the periods of negative torque when stimulation commenced too early, and matched the delay between stimulation commencement and torque rise for all trials. After the initial rise, measured and modelled data did not match as well. The rate of rise in crank torque differed between the model and individual results, as did the crank angle where torque reached its maximum. The most likely explanation for these differences lies in the over-simplification of modelling gluteus maximus as a single muscle fibre. This over-simplification prevented a close match between measured and modelled hip extension torques in Section 6.2.2 and thus is likely to have had similar effects on the amount of torque applied to the cycle crank in response to active hip extension.

Analysis of the changes in power output with stimulation firing angles for those subjects that did produce measurable torques revealed no obvious angles that maximised power applied to the cranks. Although the measured results were equivocal, the model matched the initial rise in crank torque including the cross-over from negative to positive torque. It therefore seems likely that the model could adequately predict stimulation firing angles for the gluteal muscles. This result cannot, however, be confirmed from the present results. The NMES firing angles for gluteus maximus predicted by the model to result in maximum power output were 273 to 85 deg. These angles were consistent across subjects because anthropometric differences did not significantly alter the crank angles at which the hip began to flex and extend. Although there was considerable difference between individuals in the pattern of torque production, this would not be expected to affect peak gluteus maximus firing angles by

a significant degree. Firing angles to maximise acute power output are dependent primarily on the range of crank angles through which the muscle shortens, and not by the pattern of torque production within this range.

7.5 The effect of seat position on NMES firing angles

7.5.1 Amount of movement

The angle seeking experiments described in Sections 7.2 to 7.4 were repeated on a subsequent day with the seat moved further back from the crank axle. It was planned to move the seat back by 5 cm between the seat forward and seat back conditions, however three subjects could not move the seat back without fully extending the knees while cycling. The mean distance moved by the seat was 3.6 cm. Analysis of the digitised video data revealed that the mean distance from axle to hip only changed by 2.8 cm, suggesting that the subjects changed their position on the chair as it moved back. While this distance seems rather small, Figure 7.5.2.2 demonstrates that the range of knee angles changed substantially for some subjects.

7.5.2 Quadriceps and gluteal muscles.

For the seat-back position, stimulation angles resulting in maximum power output were determined from the angle-seeking experiments using regression analyses similar to Sections 7.2 to 7.4 . Full results from these analyses may be found in Appendix 4.2.2. With the quadriceps and gluteal muscles, there was little change in peak stimulation firing angles when the ergometer seat was moved back (Figure 7.5.2.1, Table 7.5.2.1). Measurements of gluteal cessation angles were hampered by very large uncertainty in the measurement. When this uncertainty is taken into account, there is no suggestion from the available data that the stimulation firing angles resulting in peak power output changed with seat position on the current ergometer.

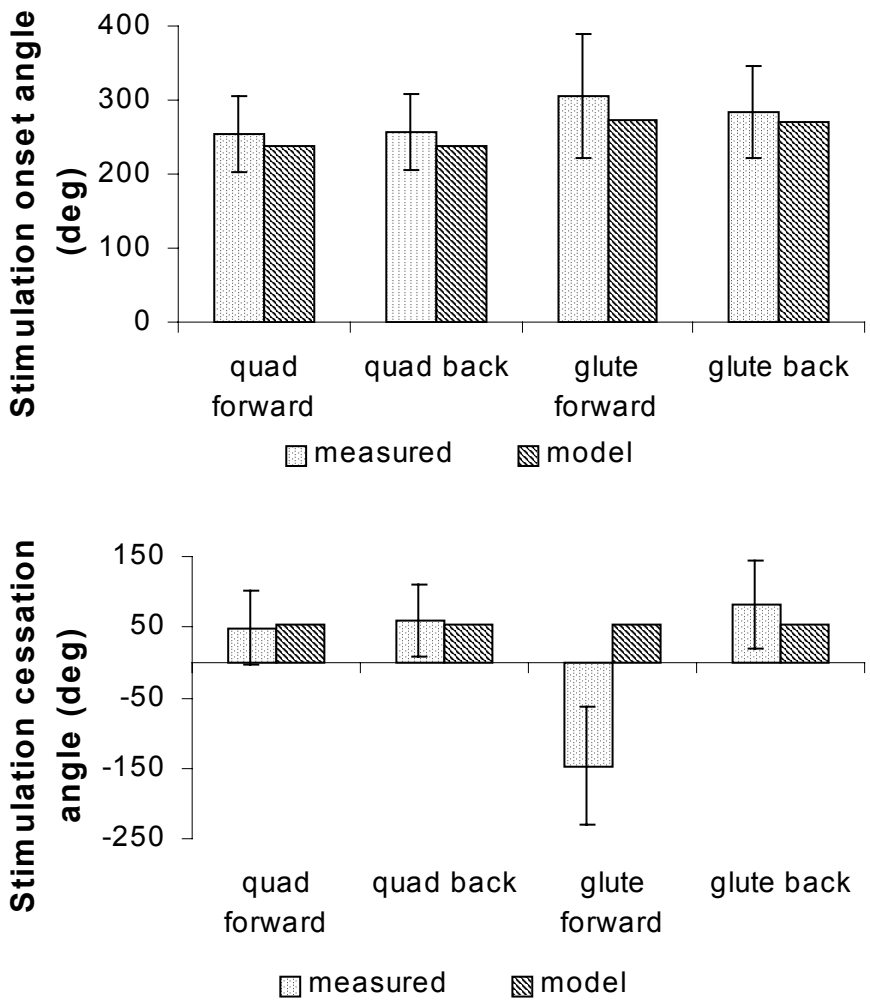

Figure 7.5.2.1 The effect of seat position on NMES firing angles for quadriceps and gluteal muscles measured from regression analyses.

Table 7.5.2.1 Comparison between measured and modelled firing angles for quadriceps and gluteal muscles.

			Model angle	Measured angle	Measurement uncertainty*
on	Quadriceps	Forward	237	254	52
		Back	238	256	52
	Gluteals	Forward	274	306	84
		Back	271	283	62
off	Quadriceps	Forward	53	49	15
		Back	55	60	17
	Gluteals	Forward	53	-147	365
		Back	55	82	117

* Uncertainty averaged from uncertainty due to constants a and b.

Section 7.3.4 suggests that optimum firing angles are dependent on the crank angles where the muscle begins to shorten, together with some allowance for activation time. The quadriceps behave as a single joint muscle because of the small relative size of the rectus femoris component; hence both quadriceps and gluteal muscles should be expected to demonstrate peak firing angles at crank angles relative to the commencement of knee and hip extension respectively. Figures 7.5.2.2 and 7.5.2.3 indicate that, while changing the seat position affected the range of motion of the hip and knee, the crank angles at which the hip and knee first began to extend remained unaltered. This explains why the peak firing angles remained constant with seat position.

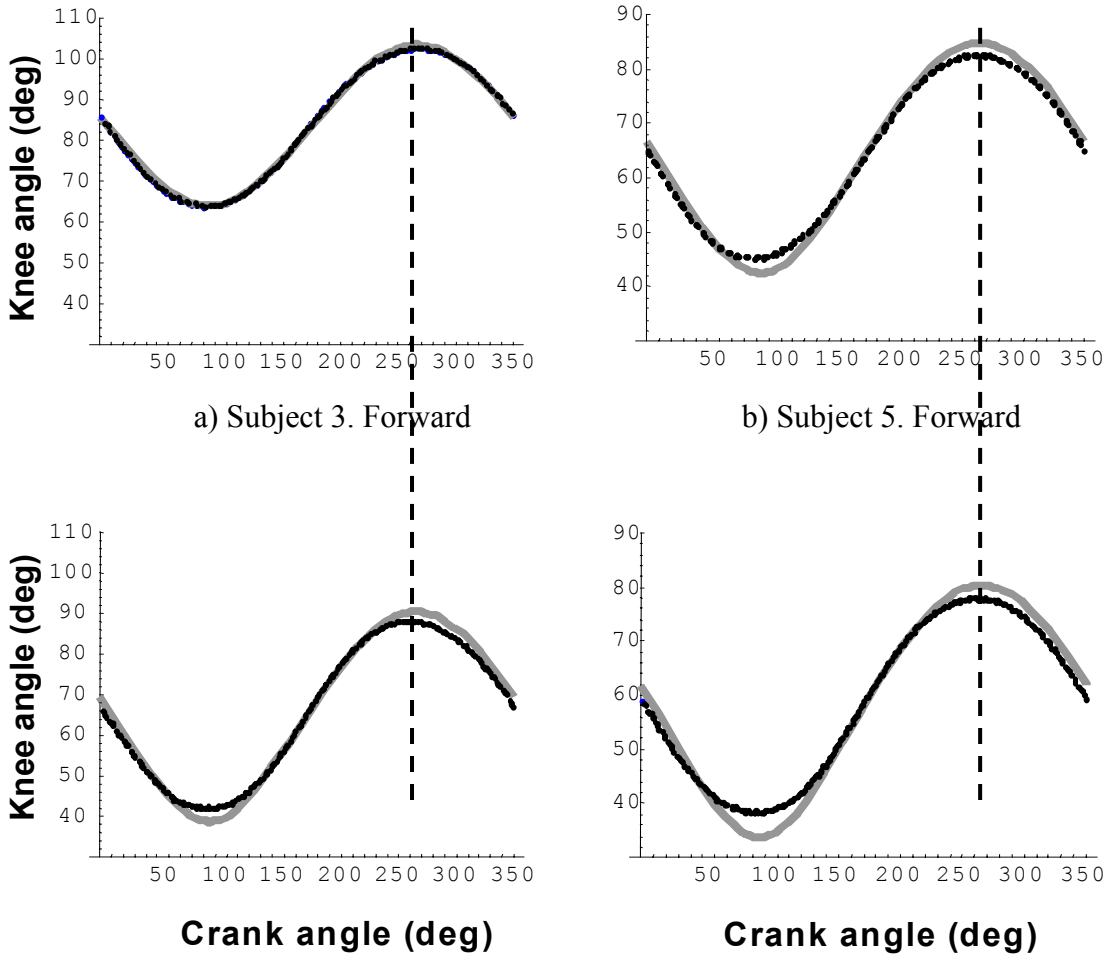

a) Subject 3. Forward

b) Subject 5. Forward

c) Subject 3. Back

d) Subject 5. Back

Figure 7.5.2.2 Effect of seat position on measured and modelled knee angles for two exemplar subjects. Solid grey lines are modelled angles; dotted black lines are angles measured from video film.

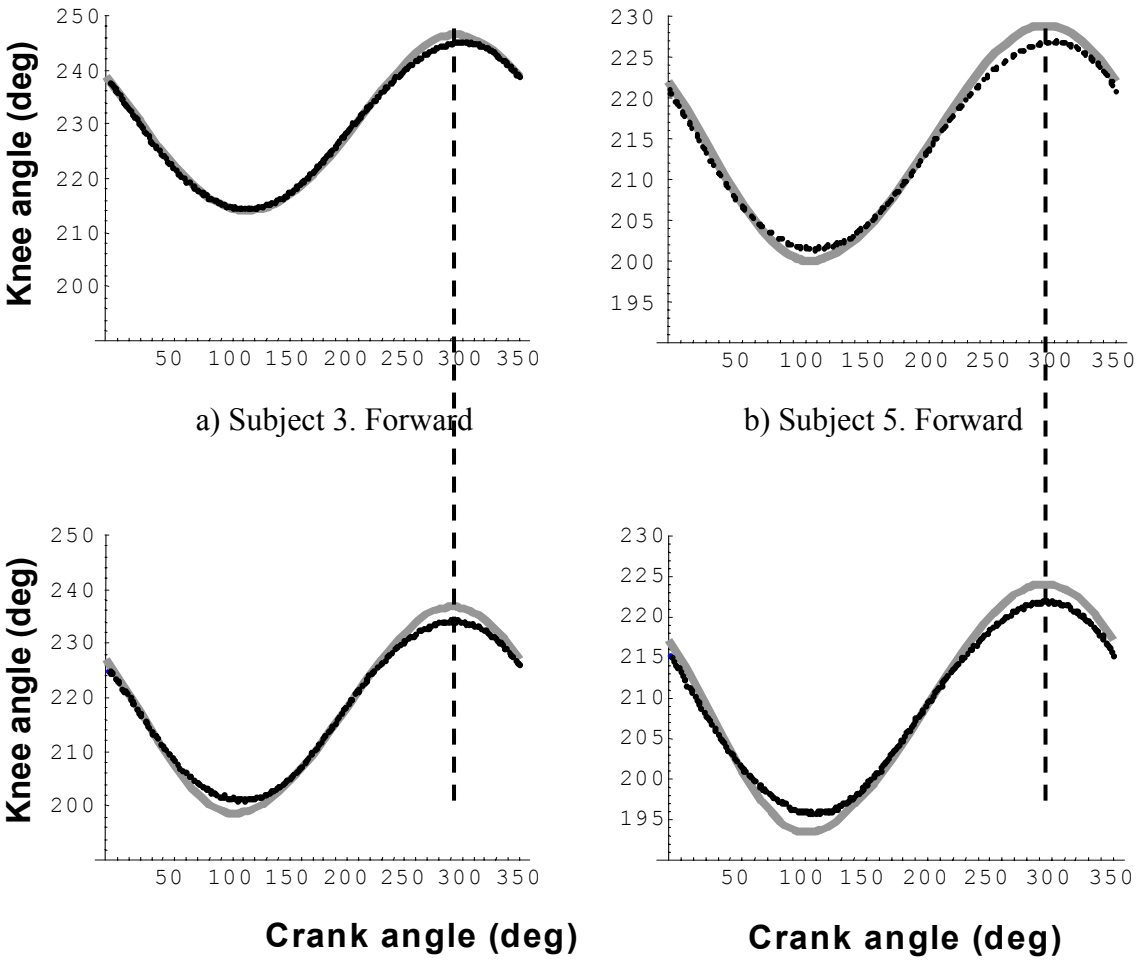

a) Subject 3. Forward

b) Subject 5. Forward

c) Subject 3. Back

d) Subject 5. Back

Figure 7.5.2.3 Effect of seat position on measured and modelled thigh angles for two exemplar subjects. Solid lines are modelled angles; dotted lines are angles measured from video film.

7.5.3 Hamstring muscles.

Comparisons between forward and back seat positions on hamstring firing angles were difficult because of the variability in response between subjects and the high uncertainty in measuring individual responses. Visual inspection of Figure 7.5.3.1 suggests that moving the seat back had a different effect on each subject; with subjects either increasing peak stimulation onset angle, decreasing or remaining similar.

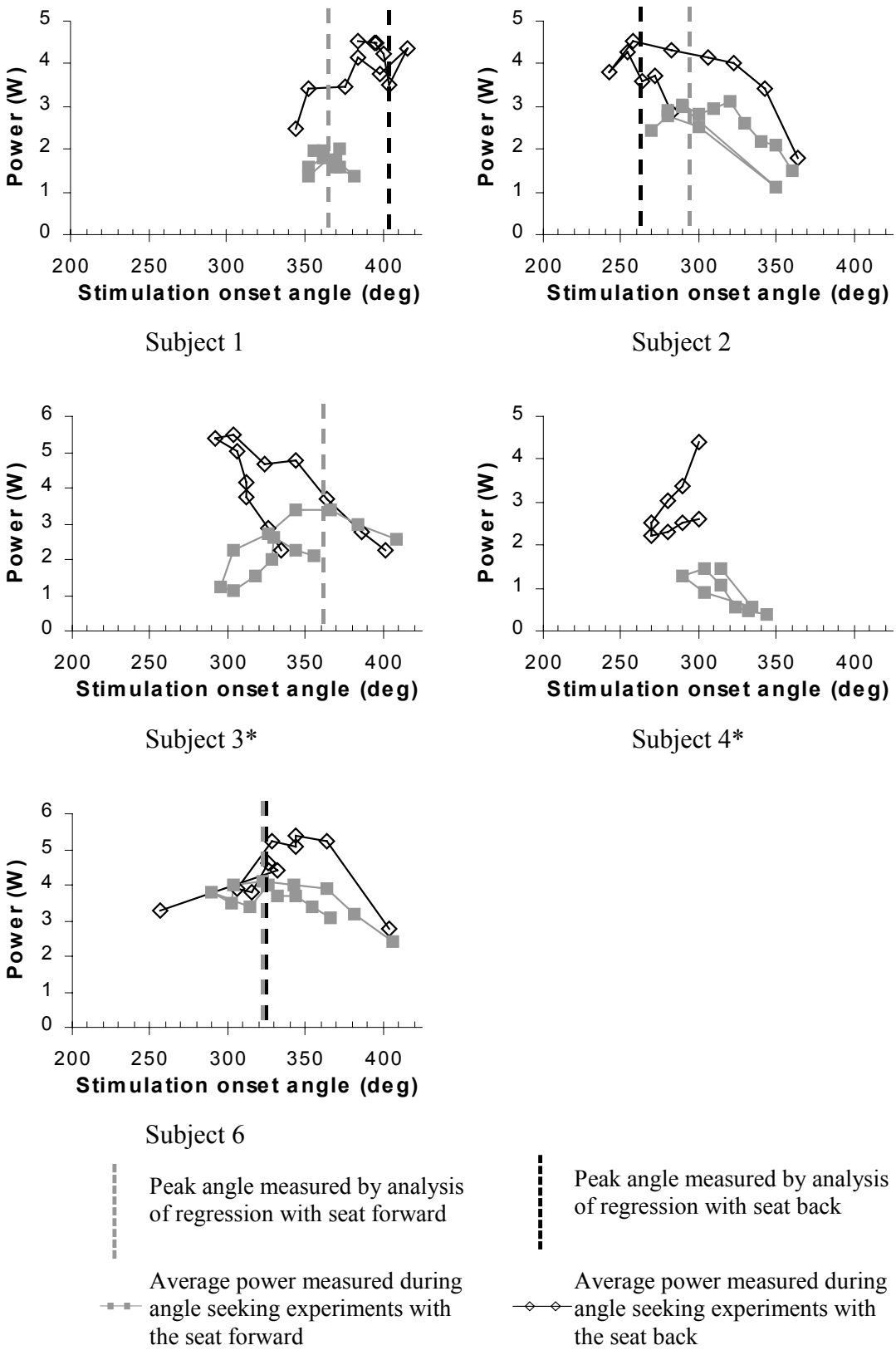

Figure 7.5.3.1 A comparison between NMES onset angles that maximise measured power output by the hamstring muscles at two seat positions.

* Regression analysis was unable to find a maximum value within the range of angles measured for these 2 subjects.

Hamstring knee moment arms were again modified to improve the match between measured and modelled pedal forces using hamstring stimulation onset angle of 0 deg. Changing the knee moment arms by an average of 17% resulted in an improvement in correlations between measured and modelled crank torques from 0.47 with standard moment arms to 0.67 with modified moment arms.

Table 7.5.3.1 shows a comparison of the moment arm modifications made using data from 2 separate days of testing with the seat forward and back. While there is some agreement between moment arms modified using the 2 separate days testing, the relationship is only moderate ($r = 0.71$). This supports the hypothesis that inter-subject differences in peak stimulation angles are due, at least in part, to inter-subject differences in the relative hip-knee moment arms. If the adjusted moment arms were correct, however, they should have been calculated to be the same on each day of testing. The differences in required modifications may be a reflection on the method by which moment arm ratios were estimated. Other factors such as measurement error, pelvis angle, electrode placement, etc would also have influenced the model's performance, and moment arms may have been altered to compensate in part for these errors as well as real moment arm differences. Estimates could probably be improved if moment arms were adjusted to fit a range of trials simultaneously, rather than fitting moment arms to a single trial on each day; however an experiment designed specifically to measure relative hip-knee moment arms would be preferred.

Table 7.5.3.1 Hamstring knee moment arm modification ratios calculated from seat forward and seat back positions.

Subject	Seat Forward	Seat back
1	125%	145%
2	60%	80%
3	100%	80%
4	60%	95%
5	70%	*
6	85%	90%

* Insufficient torque generated for this subject to match modelled data

Hamstring moment arm adjustment improved the prediction ability of the model in the seat back position similarly to the seat forward position (Figure 7.5.3.2). Again, difficulties in identifying the true stimulation angles for peak power inhibit valid assessment of the model's performance for hamstring muscles. Visual inspection of Figure 7.5.3.2 suggests, however, that the model's ability to predict hamstring stimulation firing angles was improved when knee moment arms were modified.

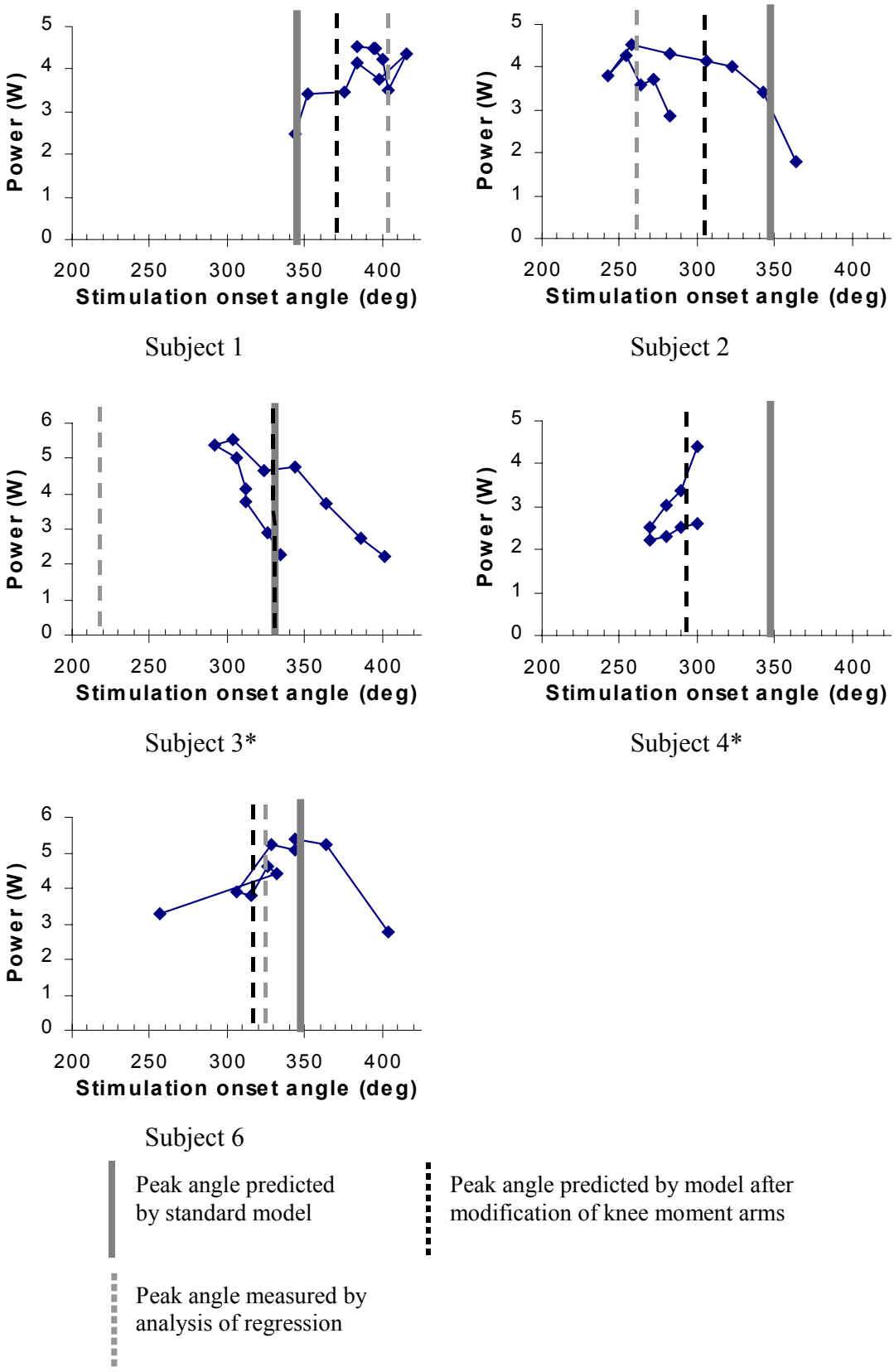

Figure 7.5.3.2 A comparison between measured and modelled NMES onset angles that maximise power output by the hamstring muscles with the chair set back.

* Regression analysis was unable to find a maximum value within the range of angles measured for these 2 subjects.

Modelling peak hamstring firing angle using the modified moment arms yielded a greater difference in firing angles between the seat forward and back positions than when standard moment arms were used (Table 7.5.3.2). This is because different moment arm modifications were used between the seat forward and back positions (Table 7.5.3.1). Had the same modifications been used in the forward and back positions, the difference between seat forward and back firing angles would have been expected to be similar to those calculated using the standard model.

Peak hamstring firing angles changed more with seat position than did quadriceps and gluteal muscles because the hamstrings are not single joint muscles. The standard model predicted stimulation onset should commence around 340 deg for all subjects in the seat forward position and around 320 deg when the seat was moved back. Figures 7.5.2.2 and 7.5.2.3 indicate that both the hip and knee were extending at these crank angles. The hamstrings generate positive work when they shorten; that is, when the product of hip velocity and moment arm at the hip is greater than the product of knee velocity and knee moment arm. Changing the seat position alters the moment arms and velocities for both joints such that the shortening action at the hip becomes greater than the knee's lengthening action at an earlier crank angle. This effect is similar to the different peak firing angles that resulted from each subjects individual hip-knee moment arm ratio.

Table 7.5.3.2 Comparison between modelled hamstring stimulation angles using both standard and modified models in two seat positions.

	Subject	Standard model		Modified model	
		Forward	Back	Forward	Back
Onset	1	330	345	371	395
Angles	2	346	347	305	315
	3	331	331	331	310
	4	341	347	293	338
	5	349	351	307	*
	6	345	347	317	331
	Mean	340	345	321	338
Cessation	1	156	171	181	202
Angles	2	166	170	132	140
	3	156	156	156	137
	4	165	156	122	163
	5	172	173	130	*
	6	168	168	152	158
	Mean	164	166	146	160

* Insufficient torque generated for this subject to match modelled data

7.5.4 Summary

Changing the seat position had little effect on peak NMES firing angles for the quadriceps and gluteal muscles. This is most likely because they both behave like single joint muscles and are only influenced by the crank angle at which their joints begin to extend. Changing seat position did not change the crank angles where maximum flexion of the hip and knee occurred; hence, there was little change in peak stimulation timing for these muscles.

Timing of hamstring muscle shortening was influenced by both the hip and knee joints. Changing seat position changed the balance of hip to knee moment arms and velocities, resulting in changes of peak firing angles. Large uncertainties in the measurement process prohibit the exact quantification of these changes, however it can be seen that changes do occur; and differently in individual subjects.

Modifying the relative balance between hip and knee moment arms for individual subjects can improve the ability of the model to predict stimulation timing patterns. Moment arm modifications made using two different days testing were not exactly the same ($r = 0.71$), indicating only a moderate reliability of this method to determine moment arms for individual subjects. It is anticipated that an experiment specifically designed to measure moment arms would be able to make more reliable estimates than the present study. The present study does, however, demonstrate the need for hamstring moment arms to be modified for individual subjects.

The amount of change in seat position for this section was relatively small compared with the differences in seat position that would be experienced when moving, for example, from one chair to another or between ergometer types. Sitting in a higher chair above the ergometer crank would be expected to have a greater effect on the crank angles at which each joint commences flexing and extending, with corresponding effects on peak NMES firing angles. This point will be explored further in Section 8.2.

7.6 Sensitivity of predicted NMES firing angles to model parameters

The sensitivity of model predictions to each variable in the model was examined using a single set of subject parameters (leg length, hip position, etc). Each variable used in the cycling model was systematically changed in order to investigate its effect on optimum stimulation firing angles predicted by the model. Variables were modified over a range of values shown in Tables 7.6.1 and 7.6.2. The range of values to be studied was chosen either from ranges of values reported in published literature or by estimating potential errors in measured variables such as thigh length and hip position. Table 7.6.1 shows the change in predicted hamstring firing angles over the range of values examined for each variable. For pelvic angle (qpel), for example, the value used for all simulations thus far was 103.8 deg. The sensitivity analysis found that increasing or decreasing this variable by 14.5 deg changed the peak stimulation onset angle by 28 deg. That is, a qpel of 89.3 deg resulted in a peak onset angle of 361 deg while a qpel of 118.3 deg predicted a peak onset angle of 333 deg. Table 7.6.2 demonstrates sensitivity of optimum firing angles for the vastii muscles for similar ranges of values. The vastus and hamstring muscles have been chosen for analysis here because they are respectively uni and bi-articular muscles.

Table 7.6.1 Sensitivity of hamstring firing angles to changes in model parameters

Variable	Model Value	Change in Model Value	Change in stimulation onset angle (deg)	Change in stimulation cessation angle (deg)
dhk	*	± 40%	87	73
dhh	*	± 40%	84	68
qpel	103.8 deg	± 14.5 deg	28	20
hx	0.283 m	± 0.05 m	12	9
ls	0.495 m	± 0.03 m	10	10
Lmth0	*	± 5%	9	3
Lfoh	0.0963 m	± 0.02 m	6	6
kth	3.3%	± 1.32%	7	4
bh	2.25 lfoh	± 0.9 lfoh	8	1
slth	0.385 m	± 0.02	7	2
tfall	48.19	± .01	1	6
Avc	50 rpm	± 2.5 rpm	4	3
Rise delay	53.13 ms	± 10 ms	6	0.6
falldelay	66.42 ms	± 10 ms	0.6	6
tris	48.02 ms	± 10 ms	5	1
lc	0.086 m	± .005 m	1	4
ecch	125 %	± 15%	1	3
hy	0.192 m	± 0.05	1	3
Pennango	11.2 deg	± 4.5 deg	1	2
lt	0.352 m	± 0.03 m	1	2
amin	1 %	0.2 – 10.2 %	1	2
ah	0.35 ffoh	0.21 – 0.35	2	0.6
ffoh	500 N	± 250 N	1	0

* Moment arms and total muscle length were calculated as functions of joint angles. To investigate changes in these variables, the entire function was multiplied by a constant percentage at all joint angles.

Table 7.6.2 Sensitivity of quadriceps firing angles to changes in model parameters

Variable	Model Value	Change in Model Value	Change in stimulation onset angle (deg)	Change in stimulation cessation angle (deg)
hy	0.192 m	± 0.05	10	8
ktv	3.3%	± 1.32%	7	2
falldelay	66.42 ms	± 10 ms	2	7
Avc	50 rpm	± 2.5 rpm	3	5
dvk	*	± 40%	6	2
Rise delay	53.13 ms	± 10 ms	7	0.6
tfall	48.19	± 0.01	0.6	7
tris	48.02 ms	± 10 ms	6	1
bv	2.25 lfov	± 0.9 lfov	3	4
Lmtv0	*	± 5%	3	0.6
Pennango	9 deg	± 3.6 deg	2	1
lt	0.352 m	± 0.03 m	2	1
hx	0.283 m	± 0.05 m	2	1
lc	0.086 m	± 0.005 m	0	2
sltv	0.1556 m	± 0.012 m	1	0.6
Lfov	0.0852 m	0.080** – 0.105 m	1	0.6
ls	0.495 m	± 0.03 m	0.6	0.6
av	0.35 ffov	0.21 – 0.35	0.6	0
ffov	500 N	± 250 N	0	0.6
eccv	125 %	± 15%	0	1
amin	1 %	0.2 – 10.2 %	0.6	0.6
qpel	103.8 deg	± 14.5 deg	0	0

* Moment arms and total muscle length were calculated as functions of joint angles. To investigate changes in these variables, the entire function was multiplied by a constant percentage at all joint angles.

** Model would not run with fibre length less than 0.08 m

It can be seen from Table 7.6.1 that the hip and knee moment arms have the greatest effect on predicted hamstring stimulation firing angles. This finding is consistent with the discussion in Section 7.3 that relative hip-knee moment arms affect the crank angles where the hamstrings begin to shorten and lengthen. The relatively large uncertainty in moment arms (± 40%) may also contribute to the sensitivity of the hamstring model to moment arm values compared to other variables. For the vastus muscles, however, the model is relatively insensitive to moment arm changes (Table 7.6.2). This is because, for single joint muscles, the timing of commencement of muscle shortening is not altered by moment arm changes.

Modelled hamstring stimulation firing angles are relatively sensitive to changes in qpel (Table 7.6.1). This finding, although initially surprising, should have been expected because of the effect of pelvis angle on hip moment arm. Changing the fixed pelvis angle to extend the hip would effectively increase the modelled hip moment arm during a simulation. This would therefore have the same effect as changing hip moment arm directly.

Pelvis angle was set parallel to seat back angle for all models, owing to the difficulty in measuring pelvis position directly for each subject. Pelvis angle may therefore explain differences in both inter and intra-subject hamstring moment arms estimated in sections 7.3.1 and 7.5.3. If each subject adopted a slightly different posture in the chair, this would have resulted in differing pelvis angles with consequent changes in peak stimulation firing angles. In this case, modifying the absolute knee or hip moment arm for each subject would have compensated for changes in hip moment arm resulting from an inaccurately modelled pelvis angle. Similarly, if subjects adopted a slightly different posture at each session, this could account for the difference in modified moment arms during the two sessions discussed in Section 7.5.3. Pelvic angle had no effect on vastus timing because the angles of the thigh and shank were not affected at all by pelvic angle.

Changing horizontal hip position and shank length by 5 cm and 3 cm respectively changed hamstring stimulation firing times by approximately 10 deg because the crank angles at which the knee began to initially flex and extend were altered. By contrast, the hamstring model was relatively insensitive to vertical hip position and thigh length. This situation was reversed for the vastus muscles, with stimulation timing being more dependent upon vertical hip position than horizontal. It is likely that with a different seat configuration; for example a more upright

cycle ergometer with the hip above the crank rather than behind, the relative importance of these may be reversed.

Increasing tendon stiffness resulted in a later optimum stimulation onset for the hamstrings and vastii of 7 and 9 degrees respectively. This occurred because, as tendon stiffness increased, the muscle was able to develop tendon force more quickly. Consequently, if constant stimulation timing were maintained, a stiffer tendon would have a greater negative area under the crank torque-angle curve. Figure 7.6.1 illustrates this effect using two example tendon stiffnesses, 2% and 4.6%, chosen as the maximum range of values anticipated in Table 7.6.1. Switching the muscle with the stiffer tendon on slightly later would reduce the size of this negative area, and hence increase overall power output.

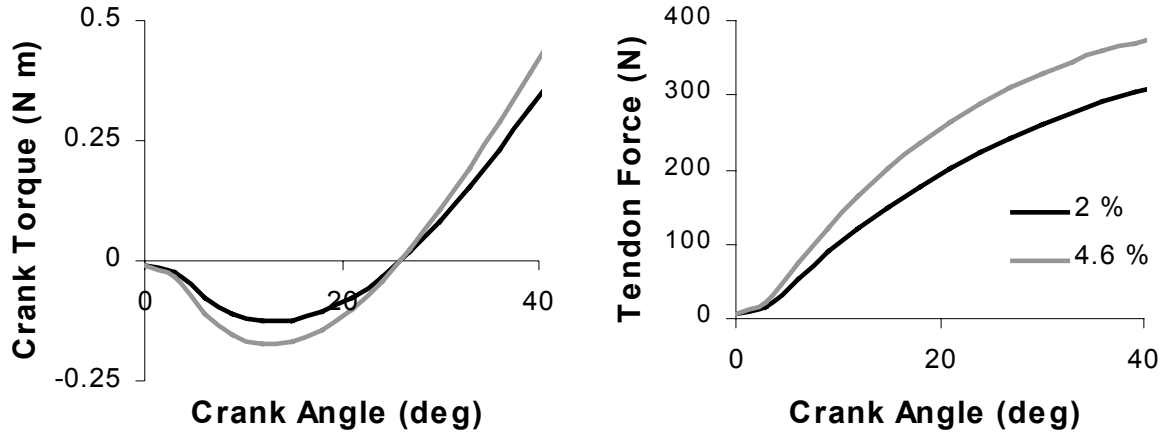

a) Crank Torque b) Tendon Force

Figure 7.6.1 Effect of tendon stiffness on the rise of tendon force and crank torque in response to NMES. The numbers 2% and 4.6% represent two modelled values for tendon stiffness.

The linear tendon force-length relationship was selected on the recommendation of Zajac (1989), owing to the relative error in measuring tendon compliance at very low force levels. This linear relationship can be criticised as being non-physiological, hence a further simulation test was performed using a non-linear relationship in order to investigate the effect

of the linear assumption. van Soest and Bobbert (1993) reported the following non linear equation, converted to use symbols consistent with the present model:

$$ft[t] = kt\left(lt[t] - slt\right)^2$$

$$\text{where} \quad kt = \frac{ffo}{\left(U_{max} \times slt\right)^2}$$

Equation 7.5.4.1

U_{max} was a term describing the relative elongation of the tendon at maximum force and was set to 0.04. Simulations were performed to investigate the effect of changing from the linear to the non-linear tendon stiffness equations. Using Equation 7.5.4.1 in place of the original linear equation changed the optimum vastus angles of both onset and cessation by 0.6 deg. For the hamstring muscles, the non-linear equation changed optimum onset angle by 0.6 deg and had no effect on cessation angle. It can therefore be seen that the assumption of linearity has very little effect on modelled outcomes when compared to assumptions about the slope of the stiffness equation.

This sensitivity analysis shows the effect of anticipated *errors* in model variables, not the full range of possible values. If seat position were changed dramatically from behind cranks to directly above, the effect on firing angles would be large. Similarly, while a 10% change in crank velocity changed stimulation onset and cessation angles by 4 and 3 deg respectively, much larger changes in velocity are possible and would result in larger changes in firing angles. The purpose of this analysis was to explore reasonable errors in the current simulations, not to describe the full effect on stimulation timing of changing cycling conditions.

Only the sensitivity of predicted stimulation timing has been investigated here. Not all kinetic outcomes have been investigated. Changing ffoh by 50%, for example, had almost no effect on stimulation timing, but would obviously change the magnitude of crank torques by a large amount. Similarly, while hy had little effect on hamstring timing, it was shown in Section 7.2.2 that the direction of vertical forces applied to the pedals was quite sensitive to changes in hy. Stimulation firing angles were the primary focus of the present modelling; hence, only these have been investigated. To investigate the sensitivity of every kinetic outcome to every model assumption is beyond the scope of the present investigation. If the present model were

used for different purposes, for example to maximise power output by adjusting seat position and angle of inclination, then sensitivity to model assumptions of the calculated power output would have to be made.